TAMPEREEN TEKNILLINEN YLIOPISTO
TAMPERE UNIVERSITY OF TECHNOLOGY

TEEMU VÄYRYNEN

MASS FLOW ESTIMATION IN MINERAL PROCESSING APPLICATIONS

Master of Science Thesis

Examiner: Professor Matti Vilkko
Examiner and topic approved in the Faculty of Engineering Sciences departmental meeting on 6 February 2013.

ABSTRACT

TAMPERE UNIVERSITY OF TECHNOLOGY
Master's Degree Programme in Automation Engineering
VÄYRYNEN, TEEMU: Mass flow estimation in mineral processing applications
Master of Science Thesis, 56 pages, 10 appendix pages
March 2013
Major: Process Automation
Examiner: Professor Matti Vilkko
Keywords: Mass flow, estimation, mineral processing, sensor

Development and implementation of automated monitoring, control and optimization systems for mineral processing applications require accurate online mass flow measurements from the processes. The mass flow sensors used in mineral processing plants are designed to monitor the production volumes of the end products.

Belt scale is the most common online bulk material mass flow sensor used in the mineral processing. The belt scale provides an accurate online mass flow measurement from the process. However, the high unit price of the sensor prevents the installation of multiple belt scales in a single mineral processing plant. In addition to the online mass flow measurements of the belt scales, offline mass flow measurements might be also carried out at the plants. Offline mass flow sensors include wheel loader scales and truck scales. The high unit price, low measurement frequency and variable measurement delays prevent the offline mass flow sensors to be used in automated process control.

The main goals of this work are determined by the three research questions formulated for this work. The first goal is to analyse the correlations of four measurement signals of the online mass flow sensors against the reference mass flow measurement of the belt scale. The fitting of the measurement signals is performed by linear regression method. The analysis of the signals is performed by measures of fit methods, the root mean square RMSE and correlation analysis method R-squared. The second goal is to analyse the accuracies of three mass flow estimation models. The third goal is to perform comprehensive analysis of the features, benefits and restrictions of each online mass flow sensor. This analysis can be utilized, if the presented online mass flow sensors are implemented in a mineral processing plant. The online mass flow sensors used in this work are a power transducer, laser profilometer, ultrasonic sensor and strain gauge.

In order to answer the research questions, an experimental measurement setup was designed and installed at the test plant. An aggregate production plant is used as an example of mineral processing application in this work. The presented online mass flow sensors can also be applied to other mineral processing applications handling solid materials on belt conveyors.

The results of this work indicate that all of the measurement signals of the online mass flow sensors correlate well with the reference mass flow measurement of the belt scale. The mass flow estimation models of the power transducer and laser profilometer were proven accurate. The results indicate that the online mass flow measurements can be utilized more effectively in the process control and optimization of the mineral processing plants. However, a reference mass flow measurement is required for calibration of the presented online mass flow sensors. Future research proposals are presented in the field of online mass flow estimation in mineral processing.

TIIVISTELMÄ

TAMPEREEN TEKNILLINEN YLIOPISTO
Automaatiotekniikan koulutusohjelma
VÄYRYNEN, TEEMU: Materiaalivirtojen estimointi mineraalien prosessointi sovelluksissa
Diplomityö, 56 sivua, 10 liitesivua
Maaliskuu 2013
Pääaine: Prosessiautomaatio
Tarkastaja: Professori Matti Vilkko
Avainsanat: Massavirta, estimointi, mineraalien prosessointi, anturi

Automaattisten monitorointi-, säätö- ja optimointijärjestelmien kehittäminen mineraalien prosessointi laitoksille edellyttää tarkkoja ja jatkuva-aikaisia massavirtamittauksia prosessista. Nykyisellään käytettävät massavirta-anturit on suunniteltu mittaamaan mineraalien prosessointilaitoksen lopputuotteiden kokonaistuotantomääriä.

Hihnavaaka on yleisin käytössä oleva jatkuva-aikainen kiinteiden materiaalien massavirta-anturi. Hihnavaa'alla saavutetaan tarkka ja jatkuva-aikainen massavirtamittaus prosessista. Sen korkea hankintahinta kuitenkin estää useiden hihnavaakojen asentamisen yksittäiseen tuotantolaitokseen. Jatkuva-aikaisten massavirtamittausten ohella voidaan suorittaa myös diskreettejä tuotantomäärien mittauksia. Yleisesti käytettyjä diskreettejä tuotantomäärien mittausantureita ovat kauhakuormaajiin asennetut vaa'at sekä rekkavaa'at. Näiden järjestelmien korkea hankintahinta, alhainen mittaustaajuus sekä pitkät ja muuttuvat viiveet estävät niiden käytön automaattisessa prosessin ohjauksessa.

Tämän työn päätavoitteet on määritetty kolmen tutkimuskysymyksen avulla. Ensimmäinen tavoite on analysoida neljän eri jatkuva-aikaisen massavirta-anturin mittaussignaalien korreloituvuutta referenssimittauksena toimivan hihnavaa'an kanssa. Mittaussignaalien sovitus tilastollista analyysia varten tehdään lineaarisella regressiolla. Tulosten analysointi suoritetaan tilastollisilla menetelmillä, joita ovat neliösumman keskivirhe (RMSE) sekä signaalien korreloituvuutta kuvaava R^2. Työn toinen tavoite on analysoida esitettyjen massavirtojen estimointimallien tarkkuutta. Kolmas tavoite on tehdä kattava analyysi eri jatkuva-aikaisten massavirta-antureiden ominaisuuksista, eduista sekä rajoituksista. Tätä analyysiä voidaan käyttää hyväksi tulevaisuudessa, jos esitettyjä jatkuva-aikaisia massavirta-antureita asennetaan mineraalien prosessointilaitoksiin. Tässä työssä käytettävät jatkuva-aikaiset massavirta-anturit ovat tehonmuunnin, laserprofilometri, ultraäänianturi sekä venymäliuska.

Jotta tässä työssä määritetyille tutkimuskysymyksille voidaan löytää vastauksia, työssä käytettävälle testilaitokselle suunniteltiin ja rakennettiin kokeellinen massavirtojen mittausjärjestelmä. Esimerkkinä mineraalien prosessointisovelluksesta käytetään testilaitoksena toimivaa kivenmurskausprosessia. Tutkittuja massavirta-antureita voidaan käyttää myös muissa kiinteitä materiaaleja käsittelevissä mineraalien prosessointilaitoksissa.

Tämän työn tulokset osoittavat että kaikkien käytettyjen jatkuva-aikaisten massavirta-antureiden mittaussignaalit korreloivat hyvin hihnavaa'an referenssimassavirtamittauksen kanssa. Tutkitut massavirtojen estimointiteoriat osoittautuivat tarkoiksi tehonmuuntimen ja laserprofilometrin osalta. Tulokset osoittavat että jatkuva-aikaisia massavirtamittauksia voidaan käyttää nykyistä tehokkaammin hyödyksi mineraalien prosessointilaitoksien säädössä ja optimoinnissa. Jatkuva-aikaisten massavirta-antureiden kalibrointia varten tulee kuitenkin olla olemassa referenssimassavirtamittaus. Tässä työssä

esitetään myös jatkotutkimusehdotuksia liittyen jatkuva-aikaisiin massavirta-mittauksiin mineraalien prosessointilaitoksilla.

PREFACE AND ACKNOWLEDGEMENTS

This work is done for the SOREX project which is part of the Green Mining research program. The Green Mining research program is a collaboration program founded to develop new methods and technologies for mineral processing. The project is funded by Finnish Funding Agency for Technology and Innovation (Tekes), various Finnish mining industry companies and universities from Finland. This work is performed as collaboration between the Department of Automation Science and Engineering at the Tampere University of Technology and Metso Minerals Tampere. The work was done mostly at the Tampere University of Technology except the experiment performed at Metso Minerals test plant.

I wish to express my gratitude to Prof. Matti Vilkko and M.Sc. Pekka Itävuo at the Tampere University of Technology for their invaluable guidance and advice throughout the work. I would also like to thank M.Sc. Aki Taskinen for his help and previous research in the field of optical measurement methods and the laser profilometer. I express my gratitude also to the funding body of my thesis work as well as various people from Metso Corporation, Niko Lamminmäki (Metso Minerals), Tero Onnela (Metso Minerals), Mika Peltonen (Metso Minerals) and Antti Jaatinen (Metso Automation) for their guidance, opinions, new ideas and co-operation during this work. I would also like to thank the whole staff at Metso Minerals research center for sensor installations and support during the experiment phase of this work.

Tampere, March 20, 2013

Teemu Väyrynen
Satamakatu 6 C 54
33200 Tampere, Finland

CONTENTS

TERMS, DEFINITIONS, ABBREVIATIONS AND SYMBOLS

ABBREVIATIONS:

AC	Alternating current
DC	Direct current
EUPG	European Aggregates Association
FEM	Finite element model

SYMBOLS:

$\boldsymbol{A}$	Interception point of the linear regression line with the y-axis
$\boldsymbol{B}$	Slope factor of the linear regression model
$\boldsymbol{c}$	Velocity of ultrasonic pulse in the air [m/s]
$\boldsymbol{cos(\varphi)}$	Power factor of the electrical system
$\boldsymbol{D}$	Distance between the membrane of the ultrasonic sensor and the measured surface [m]
$\boldsymbol{E}$	Young's modulus [GPa]
$\boldsymbol{E}$**D**	Empty distance [m]
$\boldsymbol{g}$	Acceleration of gravity [m/s^2]
$\boldsymbol{h}$	Lifting height of the conveyor [m]
$\boldsymbol{H_{average}}$	Average material height profile [m] (vector)
$\boldsymbol{H_{conveyor}}$	Empty conveyor profile [m] (vector)
$\boldsymbol{h_{drop}}$	Drop height of the material to the conveyor [m]
$\boldsymbol{H_{material}}$	Height profile of the material subtracted with the empty conveyor profile [m] (vector)
$\boldsymbol{H_{surface}}$	Height profile of the material [m] (vector)
$\boldsymbol{I}$	Current [A]
$\boldsymbol{k}$	Gauge factor
$\boldsymbol{k_y}$	Scaling factor of the measurement in vertical direction
$\boldsymbol{k_y}$	Scaling factor of the measurement in horizontal direction [m]
$\boldsymbol{L}$	Height of the material profile [m]
$\boldsymbol{l_i}$	Distance between the belt scale rollers and the neighbouring rollers [m]
$\boldsymbol{L_{org}}$	Original length of the object [m]
$\boldsymbol{l_t}$	Measurement distance of the belt scale [m]
$\boldsymbol{\Delta L}$	Change of the length [m]
$\boldsymbol{m}$	Mass [kg]
$\boldsymbol{\dot{m}}$	Mass flow [kg/s]
$\boldsymbol{M_i}$	Mean value of signal *i*

$\boldsymbol{m_{tot}}$	Cumulative mass measurement [kg]
$\boldsymbol{n}$	Number of the measurement samples
$\boldsymbol{\eta_{tot}}$	Coefficient factor of the conveyor system [W]
$\boldsymbol{P}$	Instantaneous electrical power of the electric motor [W]
$\boldsymbol{P_{electrical}}$	Electrical power of the motor [W]
$\boldsymbol{P_{idle}}$	Idle power of the electric motor [W]
$\boldsymbol{r}$	Correlation between signals the two signals
$\boldsymbol{R^2}$	Correlation coefficient value
$\boldsymbol{R_0}$	Original resistance of the object [Ω]
$\boldsymbol{\Delta R}$	Change of resistance [Ω]
$\boldsymbol{RMSE}$	Root mean squared error
$\boldsymbol{S_i}$	Standard deviation of signal *i*
$\boldsymbol{T_{flight}}$	Time of flight of the ultrasonic pulse [s]
$\boldsymbol{U_{EX}}$	Excitation voltage of the Wheatstone bridge [V]
$\boldsymbol{U_{Li}}$	Potential difference of the phase line *i* and the zero potential [V]
$\boldsymbol{U_M}$	Measurement voltage [V]
$\boldsymbol{U_\Sigma}$	Equivalent three-phased voltage [V]
$\boldsymbol{v}$	Velocity of the conveyor belt [m/s]
$\boldsymbol{y'}$	Prediction of the linear regression model
$\boldsymbol{\overline{y}}$	Mean value of all measurement values of the mass flow sensor
$\boldsymbol{\alpha}$	Inclination angle of the conveyor system [degree]
$\boldsymbol{\varepsilon}$	Strain [dimensionless]
$\boldsymbol{\sigma}$	Stress [N/m]
$\boldsymbol{\hat{\rho}}$	Bulk density estimate of the material [kg/m^3]

1 INTRODUCTION

In mineral processing applications there is a trend to increase advanced automated process control and optimization. This trend generates new requirements for the online mass flow measurement solutions. This work analyses four methods, which are used for online mass flow measurements in mineral processing. The physical principles behind the methods are power demand of the belt conveyor, optical material height profile measurement, ultrasonic material height measurement and strain of the belt conveyor structures. The mass flow estimation methods analysed in this work are measuring mass flows from belt conveyors, which are the most common mass transfer solutions in mineral processing plants.

This chapter presents the motivation for development of online mass flow measurements and the previous research in the field. Also, the research questions and goals, and the structure of the work are presented. After reading this chapter, the reader should be aware of the scientific problem this work is focused on and can move to the following chapters which present the methods, experiment, results and conclusions.

1.1 Motivation

Comminution[1] is an essential process in mining, mineral and aggregate industries. Comminution is used in mining and mineral processing to perform pre-crushing of the raw material. Construction industry utilises comminution to produce foundation and support materials. The granular material produced by comminution is also called aggregates. Apartment foundations, roads and railways are examples of constructions that require aggregates. The most common aggregates of mineral origin are sand, gravel and crushed rock. Aggregates are usually produced from natural sources extracted from quarries and gravel pits. Also, in some countries, aggregates are produced from sea-dredged or recycled construction or demolition materials. [1]

Based on the statistics of the European Aggregates association (EUPG) for the year 2010, around 3.68 billion tons of aggregates were produced in 34 UEPG member countries. The total direct value of this production is estimated to be annually in the order of 20 billion Euros. In Europe, aggregate production industry is employing roughly 250,000 people working in over 37,000 companies, which include aggregate producers, quarries and pits. [2] The European aggregate industry has suffered dramatically from the global recession, which started in the year 2008. Comparing to the year 2006, the aggregate production volumes in Europe have declined approximately 500 million tons. More than 15,000 companies have gone out of business or consolidated, and some 150,000 people have lost their jobs in the aggregate production industry. The future

---

[1)] Comminution: action of reducing a material, especially a mineral ore, to minute particles and fragments

trends in the European aggregate production industry predict very slow or even declining general growth for the next couple of years. [2]

Traditionally, the aggregate production industry has been very conservative towards implementing new technology into their business, while operational reliability of the aggregate production equipment has been the main concern. The harsh operational environment of the process causes significant challenges and restrictions for the utilisation of measurement and automation technology. If compared to other fields of process industry, such as chemical, paper and energy production, the level of analytical process knowledge and implemented automated process control systems is relatively low.

Increasing energy prices, tightening environmental safety requirements and more demanding quality expectations of the produced aggregates are generating new challenges for the companies working in the aggregate production industry. The listed challenges and even hardening competition between the aggregate producers are forcing the companies to reconsider and modify their production methods and strategies in the near future.

A modern aggregate production plant is a combination of specialised equipment, such as crushers, screens, rock blasting equipment, transportation equipment and storages. Additional equipment, such as scrubbers and mixers can also be included [3]. The aggregate production plants can be categorised into two main types, mobile and stationary. The production plant type is chosen based on rock characteristics, plant capacity, deposit lifetime, end product mix, equipment and space availability and time constrains [4]. Aggregates have a relatively low value of 4.60-34.91 Euros per ton [5]. In the recent years, the aggregate production industry has transformed more agile, while companies have increased the number of mobile aggregate production plants. The mobile plants allow contractors to operate in a wider geographical area than the stationary plants, and therefore arise new business opportunities [6]. Figure 1.1 presents a mobile three stage aggregate production plant.

Figure 1.1. *A three stage mobile aggregate production plant.*

Depending on the end product size and shape demands, the plant can have multiple crushing stages in series called primary, secondary and tertiary. The raw material, such

as blasted rock, is fed to the primary crushing stage of the plant with a dump truck or excavator. The most common primary crusher unit is a jaw crusher while cone crushers are used in secondary and tertiary crushing stages [6]. A parallel installation of crusher units is also used to increase the overall production volumes of the plant. The different sized aggregates are separated from the material stream with screen units [6]. Efficient operation of the aggregate production plant requires maximising of the amount of high value end products, while the amount of the low value aggregates are minimised. The production ratio between different sized aggregates can be affected by operational parameters of the plant. However, choosing of the optimal parameters is hard, since there are usually no online mass flow measurements available from more than one end product conveyor of the plant [7]. An end product conveyor is presented in Figure 1.2.

Figure 1.2. *An end product conveyor of the aggregate production plant*

Aggregate production plants are under heavy wear and climate conditions during the operation. Fault situations occur often, due to component break downs, electrical failures and forced shut downs by the safety automation systems. Dust, mud, snow, water and temperature fluctuations eventually destroy most of the electrical components in the aggregate production equipment. Even keeping the equipment running requires constant maintenance and repair operations by the plant personal. The uninterrupted operation of the plant is the key priority for the companies and therefore the equipment is designed to be rugged and reliable without any unnecessary components or electronics.

Process control of the aggregate production plant can be categorised into two parts, manual process control and safety automation. The manual process control of the plant is performed by the plant operators. Control actions are performed based on measurements and visual observations from the process. However, manual control cannot overcome automated one, due to the limited observation and control capabilities of a human operator [7]. Safety automation systems are designed to keep the plant running uninterrupted and to prevent damage for the equipment. The control actions are usually on-off control of the conveyor systems and equipment.

The traditional method to improve the aggregate production, in addition to the manual control, has been the selection of the aggregate production equipment combinations.

Individual equipment, such as crusher units and screens, are combined based on the prior process knowledge of the equipment manufacturers [6]. Even though, good results have been gained with this method, the previous research indicates that better operational performance of the plants can be gained with optimization-based automated control systems [8, 9, 10].

Currently, the most common online mass flow sensor used in the aggregate production industry is the belt scale [7]. Usually only one belt scale is installed in aggregate production plant. The installation place of the belt scale is usually the main end product conveyor. From the automated process control point of view, a single belt provides accurate but too concise measurement data from the process [7]. The most significant factor which prevents the installation of multiple belt scales in aggregate production plant is the high unit price of the sensor [7]. In addition to the online mass flow measurements of the belt scales, offline mass flow measurements might be also carried out at the plants. Offline mass flow sensors include wheel loader scales and truck scales. [7]

If cost-effective and accurate online mass flow sensors were available, automated process control systems could be developed and implemented to the aggregate production processes. This is the main motivation for this work. It is very unlikely that automated process control systems become more common before the problems concerning the mass flow measurements are resolved.

1.2 State of the research

This work is not the first one that deals with the research problem described above. Numerous attempts have been carried out to increase the level of measurements and automated control in mineral processing applications. This research has been performed by academic researchers as well as companies working in the industry.

Companies, such as Metso Minerals, SICK, Vega, Berthold Technologies and Indurad perform research and product development in the field of mass flow measurements in mineral processing. The research material published by these companies, however, may include over optimistic results, when partly designed for marketing purposes. Therefore, only academic research papers are discussed in this work.

Research focusing on the process modelling indicates that major improvements in energy efficiency and production optimization of the plants could be gained by implementing more advanced automated control systems [7, 8, 9, 10, 11]. However, studies report that the control structures require accurate online mass flow measurements from multiple conveyors to work efficiently. These studies have also proved that the mass flow estimation cannot be accurately performed based on plant simulation models.

Academic and commercial research has resulted in multiple methods for online mass flow measurements. Machine vision and laser profilometer are researched as methods for mass flow measurements and particle size distribution analysis [12, 13, 14, 15]. Ultrasonic distance measurement has been used in various applications, such as aggregate production [16]. Commercialized radiation-based measurement systems can

be found for mineral processing plants [17]. Power demand measurement of the belt conveyor is possibly the most promising method available for mass flow measurements [7]. Strain gauges have been studied as independent mass flow sensors [18]. However, none of these technologies have yet managed to overcome the traditional belt scale as the standard online mass flow sensor in mineral processing applications.

If the financial and environmental scale of the mineral processing is considered worldwide, the academic research of the subject is very slim, compared to other fields of process industry. This work makes a small contribution to the research of online mass flow estimation in mineral processing.

1.3 Reseach questions and goals

The main goals of this work are formulated as three research questions described below. The first two are quantitative issues dealing with the signal correlations and accuracies of the analysed mass flow models. The third one is a qualitative issue concentrating on the factors that need to be addressed if the online mass flow sensors are used in a real life aggregate production plants. The research questions of this work are designed to analyse whether the presented sensor types are suitable for online mass flow estimation. The practical implementation and calibration methods of the online mass flow sensors are considered future research subjects and are out of this works scope.

RQ1. How accurately the measurement signals of the presented sensors correlate with the reference mass flow measurement of the belt scale?

RQ2. How accurate are the presented mass flow estimation models?

RQ3. What factors need to be considered when the sensors are used for mass flow estimation in a real life mineral processing plant?

Four sensor types are used in this work: power transducer, laser profilometer, ultrasonic sensor and strain gauge. In order to answer the research questions, an experimental mass flow measurement setup was designed and built at the test aggregate production plant during this work.

The research question number one is answered with the following procedure. First the measurement signals of the mass flow sensors are fitted to the measurement signal of the belt scale by the linear regression method. Then the correlations of the signals are analysed with measures of fit methods, the RMSE and R-squared.

The research question number two is answered by modifying the measurement signals with the mass flow models presented in this work. The cumulative errors of the mass flow estimates and the reference mass flow measurement of the belt scale are then analysed.

The research question number three is answered by evaluating multiple features of each online mass flow sensor concerning price, installation, accuracies, calibration

needs, maintenance, data transfer methods etc. An evaluation matrix of qualitative assessments is presented as a summary of the answers for the research question number three.

1.4 Structure of this thesis

This work is divided into six chapters. Chapter 2 presents the online and offline mass flow sensors used in mineral processing. Also, mass flow estimation models, linear regression and data analysing methods are presented. Chapter 3 presents a layout of the test plant and the measurement setup. A description of the experiment performed in this work is also presented. Data processing and error analysis are also presented in the subsections of Chapter 3. Quantitative and qualitative analysis is performed in Chapter 4. Chapter 4 is organized based on the research questions of this work. The first subsection answers the research question number one focusing on the signal correlation, while the second subsection concentrates on research question number two and analyses the accuracies of the mass flow estimation models. The third subsection presents answers for the research question number three concerning the qualitative features of the online mass flow sensors. Chapter 5 compares the results of this work against the research in the field of mass flow measurements and emphasizes the importance of the results of this work in a broader scientific scope. Chapter 6 concludes the whole work and proposes future research subjects.

2 METHODOLOGY

This chapter presents the sensors, mass flow estimation models, linear regression and data analysing methods used in this work. All of the sensors are presented in Subsection 2.1. The mass flow estimation models tested in this work are presented in Subsection 2.2. Subsection 2.3 introduces a general linear regression method, which is used for data analysis methods of this work. Data analysis methods are presented in Subsection 2.4.

2.1 Mass flow sensors

This subsection presents seven mass flow sensors: wheel loader scale, truck scale, belt scale, power transducer, laser profilometer, ultrasonic sensor and strain gauge. The sensors are categorised into two sections, online and offline mass flow sensors. Online sensors are capable of measuring mass flows continuously from the conveyors, while offline sensors are only capable of discrete mass flow measurement of the cumulative production volumes.

2.1.1 Offline mass flow sensors

Offline mass flow sensors, such as a wheel loader scale and a truck scale, are commonly used in the mineral processing plants. Offline mass flow measurements are performed, due to business transactions weighting requirements. Cumulative production volumes of aggregates are also measured by offline mass flow sensors. The utilisation of these sensors in automated process control as the primary mass flow sensor is not possible because of various reasons explained in Subsections 2.1.1.1 and 2.1.1.2. Offline mass flow sensors are not researched in this work, due to their unsuitability for automated process control, but are listed here because of their wide use within the mineral processing industry.

2.1.1.1 Wheel loader scale

A mobile offline mass flow sensor used in mineral processing is the hydraulic scale of a wheel loader. The basic operation principle of the scale is to measure the pressure from the hydraulic system of the bucket. Mass in the bucket generates additional pressure to the hydraulic system. The pressure measurement is converted into a mass value and integrated over the operation time of the wheel loader by an embedded system. Figure 2.1 presents a wheel loader equipped with a hydraulic scale operating with a dump truck at an aggregate production plant. [19]

Figure 2.1. *A wheel loader equipped with a hydraulic scale operating with a dump truck at an aggregate production plant.*

The most fundamental reason for installing the scale systems into the wheel loaders originates from the operational layouts of the plants. Wheel loaders are used to transport the end products to the silos, dump trucks or ships. This way, the total production volumes can be monitored during the loading operations. Also, the sufficient accuracy of approximately +/− 2 % [19], reliability and the user friendly operation has made wheel loader scale very popular within the mineral processing plants. [19]

Wheel loader scales cannot be used for automated process control due to the following reasons. Wheel loader scales have a low measurement frequency and long variable measurement delays, due to the nature of the loading operation. Other major deficiency of the wheel loader scale is that it cannot pick up and measure the entire pile of end products with one loading run. A large amount of material is left to the pile. Therefore, even with a relative fast phased loading operation of the wheel loader, the momentary measurements don’t necessarily correlate with the momentary production volumes of the plant.

2.1.1.2 Truck scale

Truck scales are rugged mechanical platforms, which measure the mass of the end products by weighting the trucks while they move through the platform [20]. The measurement is performed by weighting the mass of the truck while it enters the plant area empty and when it leaves fully loaded. The mass of the material in the truck can therefore be calculated by simple subtraction of the two masses. The operation principle of a truck scale is usually based on strain gauges or load cells. Truck scales are usually used by large stationary mineral processing plants. A truck scale is presented in Figure 2.2. [20]

Figure 2.2. *A truck scale, consisting of a weighting platform and a small operator room. [21]*

Truck scales are practical solution for large mineral processing plants, with huge production volumes and constant material flow out of the plant with trucks. They are used especially if the end products are stored in the plant area and transported out later. This way, the producer can monitor the amounts of end products when they leave the plant. Truck scale measurements can be used to charge the customers. Accuracy of a truck scale can be up to +/− 1 %, when properly installed, maintained and calibrated [20].

Truck scales cannot be used for automated control due to long and variable measurement delays caused by the operation of the plant and the transport trucks. Truck scales cannot be used even to create estimates of the produced end product amounts because of the possible storing of the end products at the plant area. However, in real life mineral processing plants truck scales have been proven reliable and easy to use by the plant operators and transportation companies as a methods for business transaction weighting.

2.1.2 Online mass flow sensors

Online mass flow sensors, such as the belt scale, power transducer, laser profilometer, ultrasonic sensor and strain gauge can perform continuous mass flow measurements from the belt conveyors. The main focus of this work are the online mass flow sensors, due to their ability to be used as part of the automated process control systems.

2.1.2.1 Belt scale

The most common mass flow sensor used in mineral production industry is the belt scale. Belt scale is usually installed in the main end product conveyor of the plant. The operation principle of the belt scale is to measure the mass on a given part of the conveyor belt with a load cell or strain gauge. The mass flow measurement of the belt scale also requires a velocity measurement of the conveyor belt. The velocity measurement is usually done by a tachometer rolling against the conveyor belt. Both mass and velocity measurements are used to obtain the mass flow value at a given time. [22]

Belt scales are accurate, when the conveyor belt is fully loaded and well maintained. The accuracy of the belt scale degreases if the conveyor belt is not fully loaded, due to the non-linear behaviour of the belt scale [7]. In order to maintain good accuracy of the belt scale, periodic calibration needs to be performed. Accuracy of a well-calibrated belt scale can be up to +/− 0.5 % [22]. This level of accuracy is practically impossible to maintain at the actual mineral processing plant, because the belt scales are very rarely calibrated [23]. The most significant problem which prevents the wider use of the belt scales in aggregate production plants is the high unit price of the belt scales [7]. Figure 2.3 presents SEG ZH13 belt scale working as the reference mass flow measurement during this work at the test plant [24].

Figure 2.3. *SEG ZH13 belt scale installed at the test plant.*

As previously presented, the operation principle of the belt scale is based on a strain gauge and a tachometer. The strain gauge measures the force, generated by the material moving on the conveyor belt, which affects the roller rack of the belt scale. The area of

the conveyor belt, which affects the measurement roller rack, depends on the distance between the roller racks. The length l_1 describes the distance from the roller rack of the belt scale to the preceding supporting roller rack, and l_2 to the succeeding supporting roller rack, correspondingly. In proper installation, both distances should be equal. The measurement distance of the belt scale l_t can be calculated with Equation 2.1. [22]

$$l_t = \frac{l_1}{2} + \frac{l_2}{2} = \frac{l_1 + l_2}{2} \tag{2.1}$$

When tachometer pulses are scaled to velocity value v of the conveyor belt, the momentary mass flow $\dot{m}$ can be calculated with Equation 2.2. [22]

$$\dot{m} = \frac{m}{l_t} v \tag{2.2}$$

Where m is the mass of the material on the measurement area. Integrating momentary mass flows over a given period of time t, the cumulative mass value m_{tot} is obtained with Equation 2.3. [22]

$$m_{tot} = \int_0^t \dot{m}(t)\, dt \tag{2.3}$$

Depending on the measurement frequency and the unit of the mass flow, a scaling factor might be required to transform the tons per hour indication to the kilograms per sample form.

2.1.2.2 Power transducer

Power transducer is an electrical sensor designed to measure main electrical variables, such as current, voltage and power from electrical systems. The utilisation of power transducer in online mass flow measurements is based on a power measurement model developed by Hulthén [7]. A brief description of the model is presented in Subsection 2.2.2.1. Power transducers are easy to implement as part of an electrical system, due to their small size and various connection options. Figure 2.4 presents Carlo Gavazzi CPT-DIN power transducer unit [25]. It is installed in an electrical cabinet of the test plant. In order to measure the current of the electrical system, a current sensor is used [26].

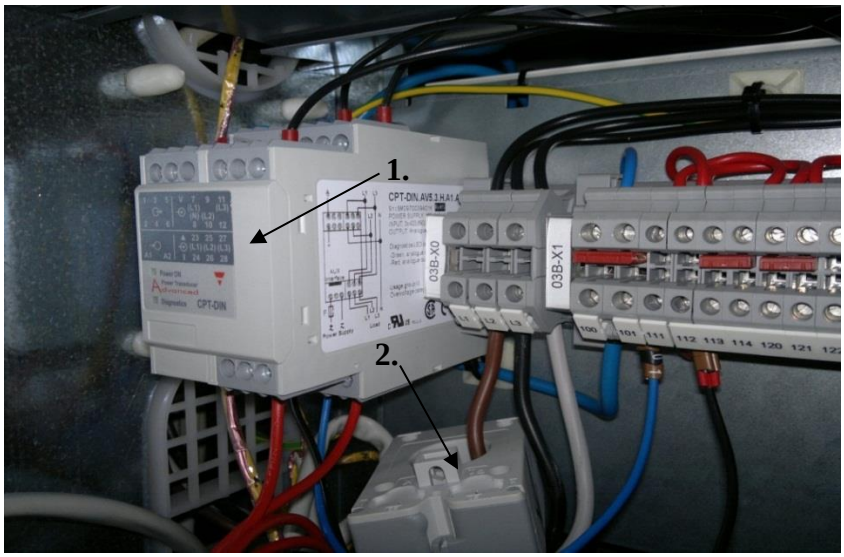

Figure 2.4. *Carlo Gavazzi CPT-DIN power transducer (1) measuring power of the three phased electric motor at the test plant. Current measurement is done with a current sensor (2) [26].*

The industrial belt conveyors are usually driven with three-phase electric motors. Therefore, the basic equations of the power measurement are presented. The power measurement of three phased electrical system requires measurements of five electrical variables, which are potential differences between the zero potential and the three phase lines, current from one of the phase lines and power factor of the electrical system. The individual potential differences are combined to an equivalent three phased voltage U_Σ presented in Equation 2.4. [25]

$$U_\Sigma = \frac{U_{L1} + U_{L2} + U_{L3}}{3} \tag{2.4}$$

Where U_{L1}, U_{L2} and U_{L3} are the potential differences between the three phase lines and the zero potential. The electrical power P in three phased AC-circuits is calculated as presented in Equation 2.5. [25]

$$P = U_\Sigma \cdot I \cos(\varphi) \tag{2.5}$$

The current value I is measured from one of the phase lines. The power factor ($cos(\varphi)$) defines the ratio between the real power flowing to the load and the apparent power in the circuit. The power factor is a dimensionless value between zero and one [27]. Integration over given time generates the total energy consumed in the system.

2.1.2.3 Laser profilometer

Laser profilometer is an optical online mass flow sensor, which utilises laser triangulation to analyse heights of objects. The laser profilometer system consists of a high speed camera, laser source and a tachometer. Figure 2.5 presents Ruler E1200 laser profilometer installed at the test plant. Ruler E1200 is a compact sensor, which integrates the laser source and high speed camera into a one unit. Laser profilometer systems can also be found equipped with a separate laser source and a camera unit. This configuration enables more variable measurement setups to be generated. [28]

Figure 2.5. *Ruler E1200 (1) installed at the test plant. Ruler E1200 has a powerful 2M class laser source (IEC 60825-1), and therefore, a cover (2) has to be used during the measurements.*

The operating principle of the laser profilometer is based on a method called laser triangulation [29]. A laser light profile is projected perpendicularly to the measured surface, and observed by a high speed camera from a specific fixed angle. While the material moves on the measured surface, the laser profile adapts to its height profile. The height value of an individual laser point is calculated based on the distance measurement and the viewing angle of the camera. Pulse triggering from the tachometer is used to calibrate the velocity changes of the conveyor belt. In order to measure the exact shape of an object or material flow volume, it is important that the distance between the height profiles is known. The operating principle of Ruler E1200 laser profilometer is presented in Figure 2.6 [30]. The individual height profiles are combined into a height value matrix with a software algorithm. The height value matrix can be used to create a 3D model of the measured object or surface. The measurement frequency of the laser profilometer is user customisable, which allows these sensors to be used in a wide range of applications. However, a high measurement frequency generates a very large amount of measurement data from the sensor. Therefore, powerful calculation algorithms are required for data processing.

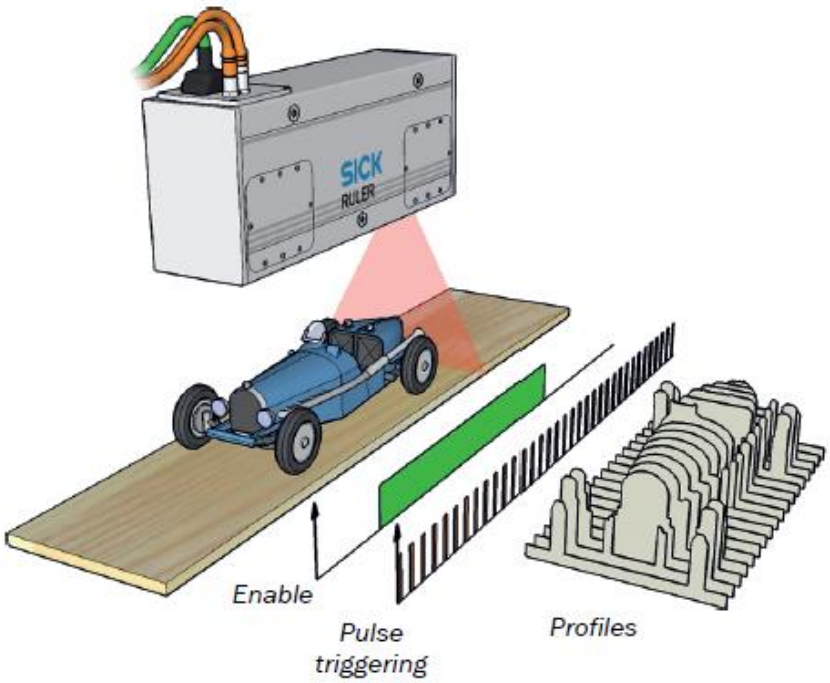

Figure 2.6. *The operating principle of Ruler E1200 laser profilometer [30]*

The field-of-view of Ruler E1200 laser profilometer is presented in Figure 2.7 [31]. Due to the optical operation principle of the laser profilometer, a stand-off area is generated in front of the sensor. Height profiles cannot be measured from the stand-off area of the camera.

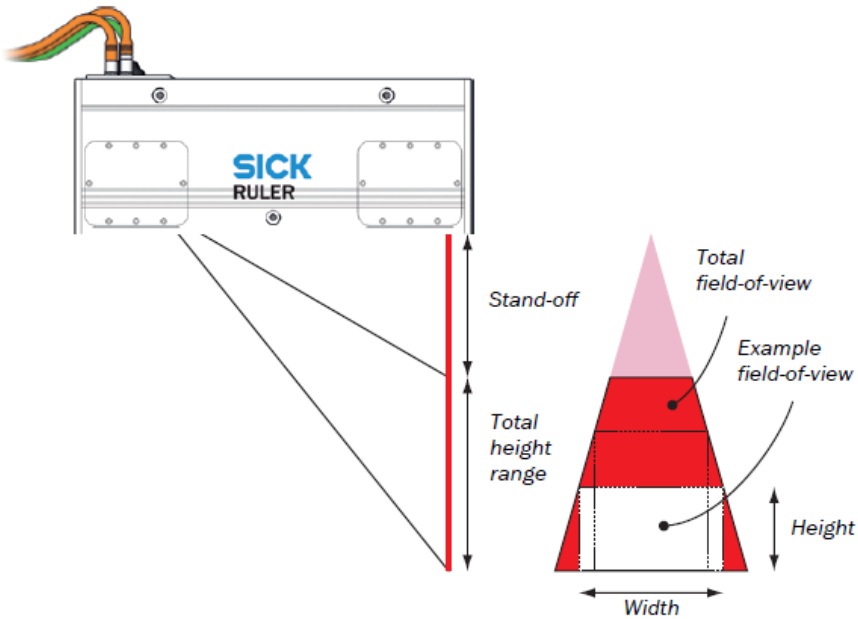

Figure 2.7. *The field-of-view of Ruler E1200 laser profilometer [31]*

As presented in Figure 2.7, the field-of-view of the laser profilometer might have blind spots due to the shape of the measured object or surface. However, a proper installation minimises the quantity and effect of these errors to the measurement signal.

2.1.2.4 Ultrasonic sensor

Ultrasonic sensor is an acoustic distance measurement sensor. Ultrasonic sensors generate high frequency sound pulses and evaluate the echoes which are received back to the sensor. The frequency of the ultrasonic sound used by the sensors is usually over 18 kHz. The sensor calculates the time interval between the sent signal and the received echo. This time interval is used to determine the distance to an object or surface. In this work, the ultrasonic sensor is used to measure height of the rock material surface moving on a belt conveyor. Figure 2.8 presents Prosonic T FMU30 ultrasonic sensor installed at the test plant. [32]

Figure 2.8. *Endress & Hauser Prosonic T FMU30 ultrasonic sensor installed at the test plant.*

The operating principle of the ultrasonic sensor is based on a measurement of the time of flight of the ultrasonic pulse. The sensor membrane transmits ultrasonic pulses to the direction of the measured surface. The ambient temperature affects the speed of the ultrasonic pulse in the air. Usually, ultrasonic sensors have internal calibration algorithms, which compensate the ambient temperature variations. When the ultrasonic pulse reaches the interface of two materials, such as air and rock, it is partly absorbed and partly reflected back. Eventually, the reflected pulses are received by the sensor membrane. The same sensor membrane may operate as a transmitter and a receiver. [32]

Given the speed of sound c in the air and the time interval T_{flight} between the sent and received pulses, the ultrasonic sensor calculates the distance D, which is the distance between the sensor membrane and the measured surface. The calculation of the distance is presented in Equation 2.6. Division by two is performed because the ultrasonic pulse travels the distance D two times before reaching the membrane of the sensor. [32]

$$D = c \cdot {}^{T_{flight}}/_{2} \tag{2.6}$$

In order to calculate the height L of the object or surface, user needs to enter an empty distance value ED to the sensor. The empty distance is the distance between the sensor membrane and the measured empty surface. The height can be calculated as presented in Equation 2.7. [32]

$$L = ED - D \tag{2.7}$$

Undesired echoes from structures may generate wrong distance measurements if the ultrasonic sensor is not equipped with a filtering algorithm. A proper installation of the ultrasonic sensor minimises the harmful interference echoes. [32]

2.1.2.5 Strain gauge

Strain gauges are used to measure strains in the objects. The most common type of strain gauge is an insulating flexible backing which includes a metallic foil pattern. The strain gauge is attached to the measured object by adhesive material. While the measured object deforms due to external force, the strain gauge is also deformed. The deformation of the strain gauge results in the change in electrical resistance of the metallic foil. The operating principle of the strain gauge can be utilised in online mass flow measurement from the belt conveyors. Figure 2.9 presents three Kyowa strain gauges installed in belt conveyor structures. The more accurate installation places of the strain gauges are presented in Figure 2.11. The strain gauges are protected with a cover against dust and rock particles. [33]

Figure 2.9. *Three Kyowa strain gauges (1) installed in the structures of the belt conveyor at the test plant.*

The strain measurement requires multiple components, such as a strain gauge element, Wheatstone bridge circuit and operation amplifier. The Wheatstone bridge circuit is an electrical circuit, designed to measure small resistant changes. Since the strains occurring in the objects can be extremely small, an operation amplifier unit is required to amplify the measurement signal. [34]

The strain gauge measures strains, which are changes in the length of the object. The unit of strain is called a microstrain. In order to perform accurate strain measurements, the strain gauge type has to be properly selected for the measured material. The most significant factor, which needs to be concerned, is the thermal expansion coefficient factor of the strain gauge element. The calculation of strain value ε in the object is presented in Equation 2.8. [34]

$$\varepsilon = \frac{\Delta L}{L_{org}} \tag{2.8}$$

Where ΔL is the change in the length and L_{org} is the original length of the object. Strain becomes a dimensionless variable. The relative change in the electrical resistance of the strain gauge is presented in Equation 2.9. [34]

$$\frac{\Delta R}{R_0} = \varepsilon \cdot k \tag{2.9}$$

Where ΔR is the resistance change of the gauge element, R_0 is the original resistance and k is a gauge factor. The gauge factor value is approximately 2.0 with the metal strain gauges. [34] Since the relationship between the strain and the resistance is known, the strain gauges can be used as part of the Wheatstone bridge. Various types of Wheatstone bridges can be found, such as the full bridge, half bridge and quarter bridge. The operating principle of the Wheatstone bridge is based on the measurement of voltage differences over the bridge. The Wheatstone bridge usually contains four equal value resistors. In the quarter bridge, one of those resistors is the strain gauge element and the three others are fixed value high precision resistors. The quarter bridge setup has all the components in the bridge, except the strain gauge which is located in the completion network. Figure 2.10 presents the general structure of the quarter Wheatstone bridge setup. [34]

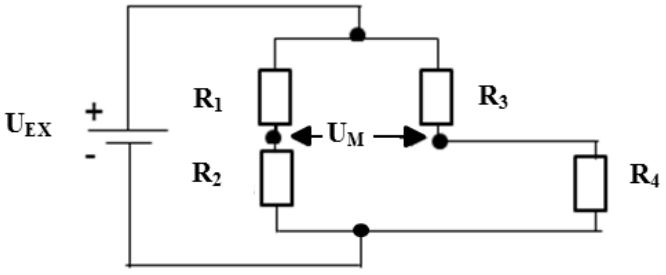

Figure 2.10. *The wiring diagram of the quarter Wheatstone bridge circuit [34]*

Where R_{SG} is the strain gauge element, R_1, R_2 and R_3 are the fixed value high precision resistors, U_M is the measurement voltage and U_{EX} is the excitation voltage (DC). The resistant change of the strain gauge is in relation to the measurement voltage, excitation voltage and strain, as presented in Equation 2.10. [34]

$$\frac{\Delta R}{R_0} = \frac{U_M}{U_{EX}} = k \cdot |\varepsilon| \tag{2.10}$$

In order to calculate the stress σ, which affects the object in the elastic deformation range, Young's modulus E of the material has to be known. Values of Young's modulus are specified for common materials and can be found in material handbooks. The unit of stress is Pascal. In this work, the data-acquisition hardware automatically converts the strain measurement values of the belt conveyor structures to stress values. The relation of the stress and strain is defined by Equation 2.11. [34]

$$\sigma = \varepsilon \cdot \mathrm{E} = \frac{\Delta R \cdot E}{R_0 \cdot k} = \frac{U_M \cdot E}{U_{EX} \cdot k} \tag{2.11}$$

The installation place of the strain gauge has a major role in the mass flow estimation capabilities of the sensor. One method to determine the optimal installation places for the strain gauges is to use structural engineering design programs. Finite element Model (FEM) theory can be used to estimate the stress and strain values in structures. [36] Figure 2.11 presents a FEM model of the conveyor roller rack, which is the installation place of the strain gauges in this work.

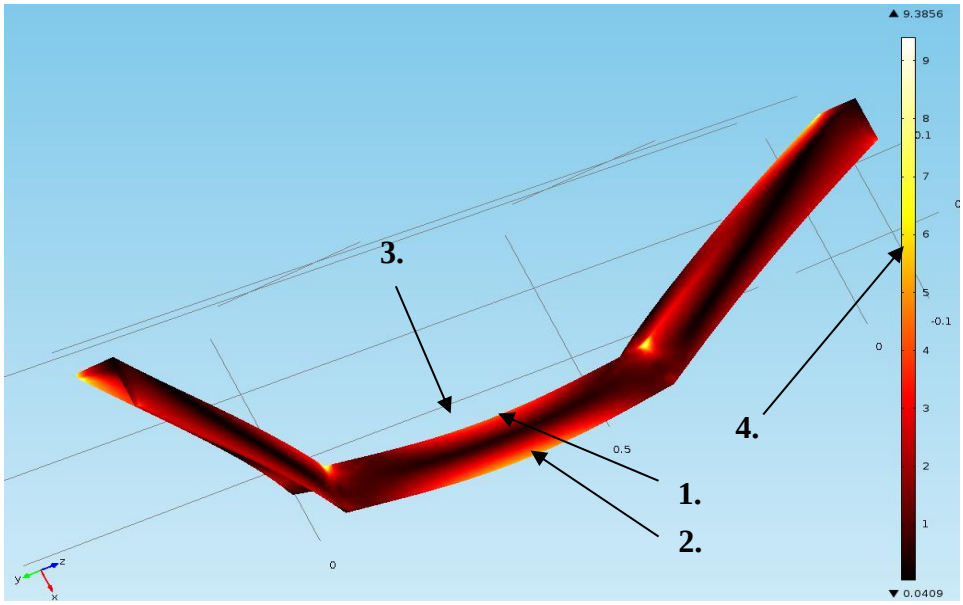

Figure 2.11. *A FEM model of the conveyor roller rack used in this work. Based on the stress estimates (4) of the simulations, the installation places for the strain gauges are determined (1, 2, 3)*

2.2 Mass flow estimation models

This subsection presents mass flow estimation models used to answer the research question number two of this work. Mass flow estimation models are presented for the power transducer, laser profilometer and ultrasonic sensor. Mass flow estimation model for the strain gauge is not presented in this work. This is because universal equation for the mass flow estimation cannot be presented, due to various types of conveyor structures and strain gauge installations. The mass flow estimation model for the power transducer is initially developed by Hulthén and modified by the author for the experiment of this work [7]. The models of the laser profilometer and the ultrasonic sensor are designed by the author.

2.2.1.1 Mass flow estimation model of the power transducer

The mass flow estimation model of the power transducer is based on the physical model of the belt conveyor. The model includes various factors, such as potential and momentum energies of the material, gravity and frictions of the belt conveyor. The mass flow is derived from calculation of two power components of the belt conveyor motor, $P_{electrical}$ which is the load dependent power and P_{idle} which is the power required to drive the empty conveyor. The presented model can only be applied to a lifting conveyor system. The parameters required for mass flow estimation with the power transducer are presented in Figure 2.12. [7]

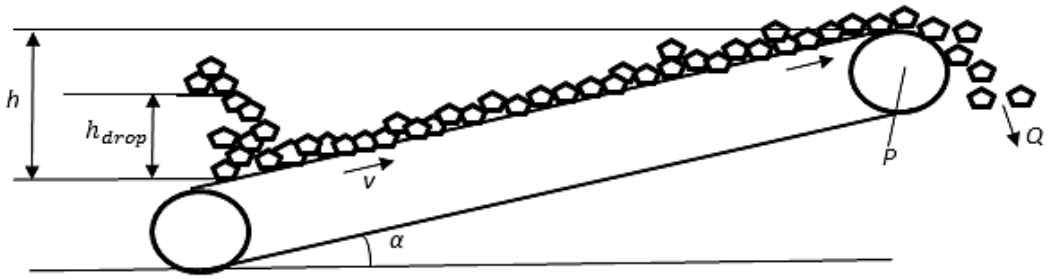

Figure 2.12. *Geometrics of a lifting conveyor system [7]*

According to the Hulthén model the mass flow on the belt conveyor can be estimated by the Equation 2.12 [7].

$$\dot{m} = \frac{(P_{electrical} - P_{idle})\eta_{tot}}{gh + v^2 + v\sqrt{2gh_{drop}}\sin(\alpha)} \tag{2.12}$$

Where η_{tot} is the coefficient factor of the belt conveyor, g is the acceleration of gravity, h is the lifting height of the belt conveyor, v is the velocity of the belt conveyor, h_{drop} is the dropping height of the material to the belt conveyor and $sin(\alpha)$ is the inclination angle of the belt conveyor. All of the parameters in the Equation 2.12, except the coefficient factor η_{tot}, can be measured. In order to generate accurate mass flow

measurements with the model, the coefficient factor has to be calculated or calibrated as Hulthén presents in his thesis work [7].

Model configuration for the experiment of this work

For the experiment of this work, the mass flow estimation model requires modifying. Since the experiment is relatively short, the drifting idle power needs to be compensated. The idle power drift is a phenomenon, which occurs for a short period of time, after the start of the material flow on a belt conveyor. The idle power will degrease during the loaded conveyor operations, due to degreasing frictions in the rollers, bearings and other components of the belt conveyor. When a specific time has passed, the idle power will reach a relatively constant value. However, in this work the idle power drifting occurs throughout the whole experiment. Therefore, the power measurement of the power transducer has a degreasing trend throughout the whole measurement data. This trend needs to be removed from the measurement in order to evaluate the real accuracy of the mass flow estimate of the power transducer.

2.2.1.2 Mass flow estimation model of the laser profilometer

The mass flow estimation model of the laser profilometer is based on the material height profile, belt conveyor velocity and geometrics, and the bulk density estimate of the material. First an empty conveyor belt height profile $H_{conveyor}$ is measured. Then, the surface height profiles $H_{surface}$ can be measured from the loaded belt conveyor. In order to generate the height profile of the material $H_{material}$, the empty conveyor profile is subtracted from the surface height profile, as presented in Equation 2.13.

$$H_{material}(x) = H_{surface}(x) - H_{conveoyr}(x) \tag{2.13}$$

When the volume flow estimate for the material is known, the mass flow estimate $\dot{m}$ can be calculated as presented in Equation 2.14.

$$\dot{m} = v\hat{\rho}\sum_{x=1}^{n} k_y k_x H_{material}(x) \tag{2.14}$$

Where v is the velocity of the belt conveyor, $\hat{\rho}$ is the bulk density estimate of the material, k_y is the height scaling factor, k_x is the conveyor belt width scaling factor for the material height profile vector and n is the amount of height measurement values in cross-direction of the conveyor belt. Figure 2.13 presents an example of the combined rock material height profiles measured with the laser profilometer.

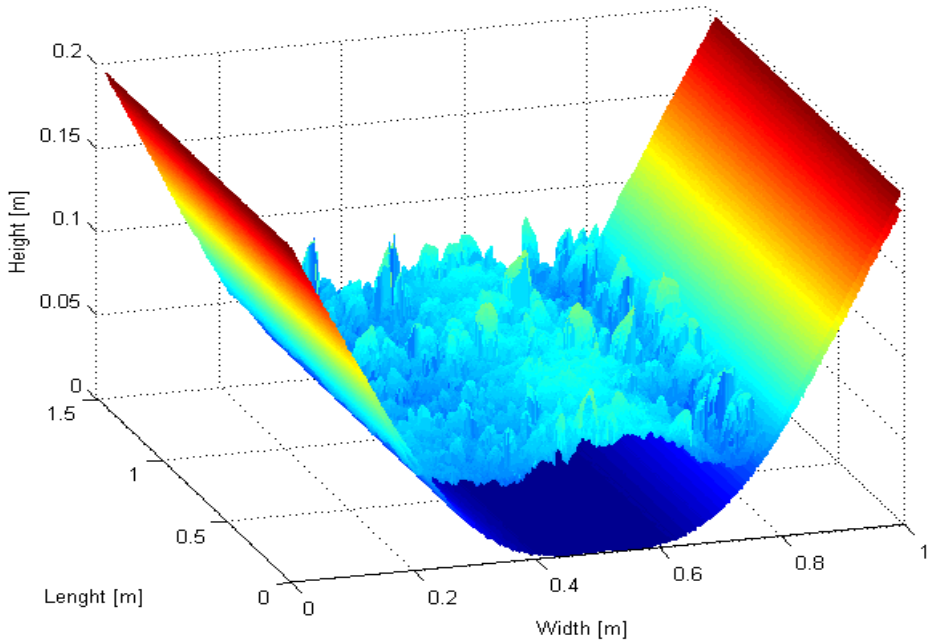

Figure 2.13. *Examples of the material height profiles and the empty conveyor measured with the laser profilometer*

Figure 2.13 has 512 height profiles taken with 500 Hz sampling frequency. Two sets of surface profiles are presented in Figure 2.13, empty and loaded conveyor belt.

2.2.1.3 Mass flow estimation model of the ultrasonic sensor

The mass flow estimation model of the ultrasonic sensor is quite similar to the one presented for the laser profilometer. Due to the operating principle of the ultrasonic sensor, the empty conveyor belt profile determination cannot be done as with the laser profilometer. Manual measurements are required from the conveyor belt. Manually measured geometrics can be used to create polynomial equation, which approximates the empty profile of the conveyor belt. Polynomial equation is presented in Equation 2.15. [32]

$$f(x) = a_n x^n + a_{n-1} x^{n-1} + \cdots + a_2 x^2 + a_1 x + a_0 \tag{2.15}$$

Figure 2.14 presents an example of the polynomial fit to a conveyor belt profile. The original conveyor belt profile is measured with the laser profilometer.

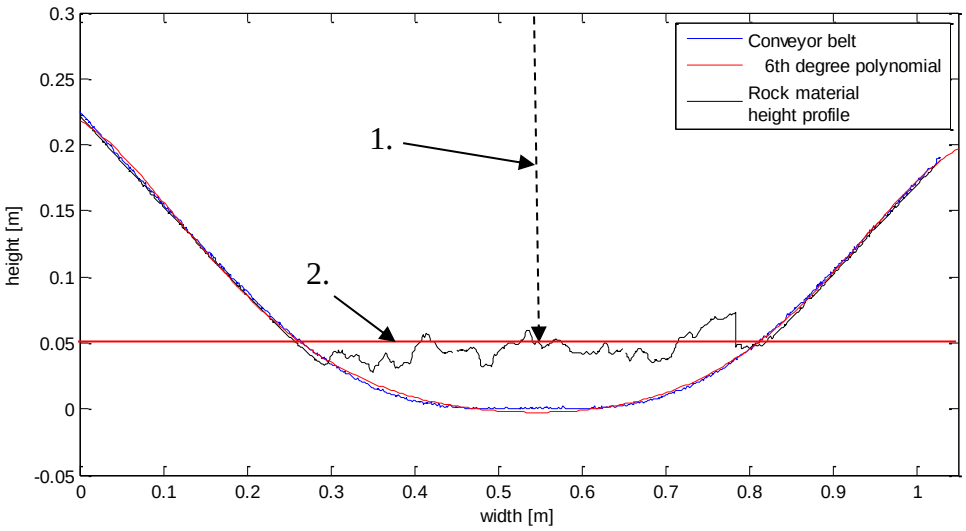

Figure 2.14. *The example conveyor belt profile is measured with the laser profilometer and 6th order polynomial is fitted to approximate the shape of the conveyor belt. The height measurement of the ultrasonic sensor (1) is used to estimate the average material profile height (2).*

The height measurement of the ultrasonic sensor is used to generate average material height profile value $H_{average}$. In order to calculate the material height profile estimate $H_{material}$, the average material height profile value is subtracted from the polynomial equation describing the shape of the empty conveyor belt. Example of the height profile approximation is presented in Figure 2.14. The calculation of the material height profile estimate is presented in Equation 2.16.

$$H_{material}(x) = H_{average} - (a_n x^n + a_{n-1} x^{n-1} + \cdots + a_2 x^2 + a_1 x + a_0) \quad (2.16)$$

Equation 2.16 generates false height values for the areas outside the intersection points of average material height value and the conveyor profile. In Figure 2.14, these areas are from 0.0 to 0.25 and from 0.82 to 1.03 meters. Equation 2.17 presents how these false height values are operated to produce correct material height profiles.

$$H_{material}(x) = \begin{cases} H_{material}(x), & H_{material}(x) \geq 0 \\ 0, & H_{material}(x) < 0 \end{cases} \quad (2.17)$$

The material mass flow estimate $\dot{m}$ is calculated based on the height profiles, the bulk density estimate of the material and the velocity of the belt conveyor. The calculation of the mass flow is presented in Equation 2.18.

$$\dot{m} = v\hat{\rho} \sum_{x=1}^{n} k_y k_x H_{material}(x) \quad (2.18)$$

Where v is the velocity of the belt conveyor, $\hat{\rho}$ is the bulk density of the material, k_y is the height scaling factor and k_x is the conveyor belt width scaling factor for the

material height profile vector. The width scaling factor is in relation to the width resolution *n* selected by the user. Figure 2.15 presents an example of the combined material height profiles, which are measured by the ultrasonic sensor from a belt conveyor. The surface profile is generated with the presented algorithm. Figure 2.15 has 16 height profiles measured with 0.8 Hz sampling frequency.

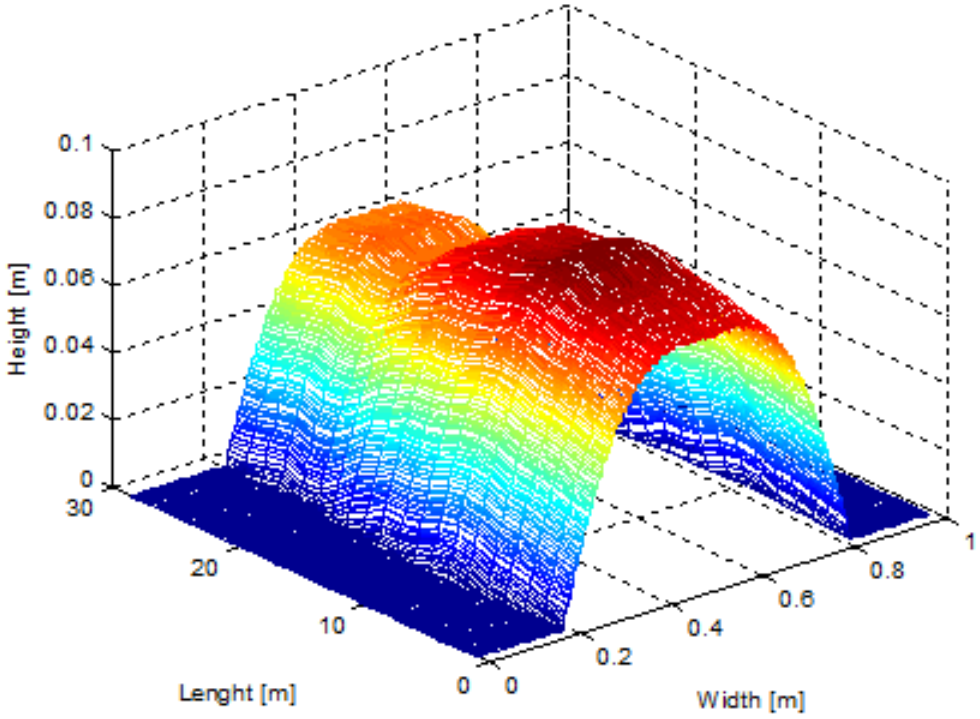

Figure 2.15. *Example of material height profile estimates, which are generated with the height measurement of the ultrasonic sensor.*

Model configuration for the experiment of this work

A compensation algorithm is required for the ultrasonic sensor in the experiment of this work. The compensation algorithm is required, due to the installation place of the sensor, which is located between the conveyor roller racks. This enables the changing of the zero level of the height measurement. Because of the operating principle of algorithm, the changing zero level causes significant errors to the mass flow estimate. The zero level changing can be compensated with an additional compensation factor k_{comp}. The quantity of the compensation factor is determined from the bending of the conveyor belt under the weight of the rock material. The compensation factor can be included in Equation 2.17 with a minor modification as presented in Equation 2.19. If the height of the material surface profile is greater than zero, then compensation factor is included.

$$H_{material}(x) = \begin{cases} H_{material}(x) + k_{comp}, & H_{material}(x) \geq 0 \\ 0, & H_{material}(x) < 0 \end{cases} \tag{2.19}$$

This procedure enables the vertical zero level compensation, without generating additional errors to the areas of the conveyor belt, which have no material.

2.3 Linear regression

This subsection presents the mathematical model of linear regression, which is used to answer the research question number one. The linear regression is used in this work to fit the raw measurement signals of the online mass flow sensors to the reference measurement signal of the belt scale. By using the linear regression method, optimal linear fitting of the measurement signals is achieved [37].

The linear regression is designed to find the best-fitting straight line through the data. The most common criterion for the best fit of the line is that the line minimizes the sum of the squared errors of the prediction. The best fitting line is called a regression line. The regression line is presented in Equation 2.20. [37]

$$y' = Bx + A \tag{2.20}$$

Where *y'* is the predicted value. The equation of the regression line consists of two linear parameters, which are the slope factor *B* of the regression line and the y-axis intercept point *A*. The parameters of the regression line are calculated based on statistical variables which are obtained from the data. The statistical parameters required for computation of the regression line are the mean values of data M_i (i denotes data sets *y* or *x*), standard deviations S_i of data and the correlation *r* between the data. The linear parameters *B* and *A* can be calculated as presented in Equations 2.21 and 2.22. [37]

$$B = \frac{r\,S_y}{S_x} \tag{2.21}$$

$$A = M_y - BM_x \tag{2.22}$$

The regression line generated by the linear regression method is the best possible linear fitting of the signals. However, due to several factors, such as nonlinearity, trends, outliers and other abnormalities in data, the prediction might not be very good throughout the data. The validation of the regression model is important to be carried out. The linear regression line, presented in Equation 2.20, is the simplest possible form of linear fitting. More complex linear regression models, containing several parameters, can also be fitted to data. In this work, only the simplest linear regression method is applied to the measurement signals. [37]

2.4 Measures of fit

This subsection presents the measures of Goodness of Fit, which are used in this work to answer the research questions number one. The linear regression models of the measurement signals are compared with the reference mass flow measurement signal of the belt scale with measures of fit. Based on measures of fit the correlations of the measurement signals can be evaluated. The data analysing methods used in this work are the root mean square error (RMSE) and the R-squared. The residual distributions of the signals are also analysed by histograms.

2.4.1 RMSE

The root mean squared error or RMSE is a quadratic method, which measures the average magnitude of the error. RMSE method calculates the momentary differences between the two signals, squares the differences and averages them over the whole data. Finally, the square root of the average error is taken. The calculation of RMSE is presented in the Equation 2.23. [38]

$$RMSE = \sqrt{\frac{\sum(x_i - y_i')^2}{n}} \tag{2.23}$$

Where x_i is the reference mass flow value of the belt scale, y_i' is the prediction of the linear regression model and n is the amount of samples in the data. The results of RMSE method can be used to evaluate the accuracy of the correlation between the linear regression models and the reference measurement signal of the belt scale. The smaller the RMSE value is, the better the correlation of the signals is. [38]

2.4.2 R-squared

The R-squared or R^2 is a Goodness of Fit method, which describe how well a regression line fits a set of data. The value of R-squared is between zero and one. If the R-squared value of data is close to one, it indicates that regression line fits the data well. If however, the value is close to zero, it indicates poor fitting of the regression line. Equation 2.24 presents the mathematic form of the R-squared. [39]

$$R^2 = 1 - \frac{\sum_{i=1}^{n}(x_i - y_i')^2}{\sum_{i=1}^{n}(x_i - \bar{y})^2} \tag{2.24}$$

Where x_i is the reference mass flow value of the belt scale, y_i' is the prediction of the linear regression model, $\bar{y}$ is the average value of all linear regression predictions and n is the amount of the measurement samples in the data. [39]

3 MEASUREMENT SETUP AND EXPERIMENT

This chapter presents the designed measurement setup and the experiment performed in this work. Sensor quantities and installation places, belt conveyor geometrics and rock material characteristics are also presented in this chapter. Data modifications, linear regression models and error analysis performed for the measurement signals are also described in detail.

3.1 Measurement setup

In order to answer the research questions numbers one and two of this work, an experimental measurement setup was designed and installed at the test plant. The measurement setup is used to compare the measurement signals of the online mass flow sensors against the reference mass flow measurement of the belt scale. The test plant used in the experiment of this work is a stationary single stage aggregate production plant. The test plant can be modified to work as an open or closed circuit. Figure 3.1 presents the layout and the equipment of the test plant as well as the installation places of the online mass flow sensors on the belt conveyor number three.

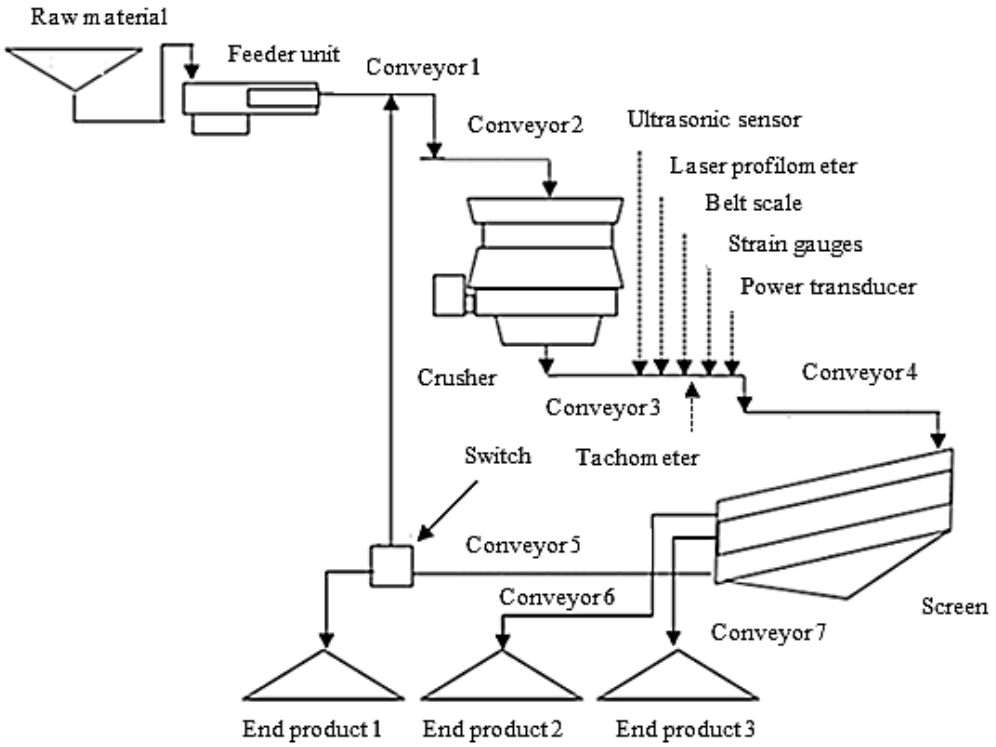

Figure 3.1. *The layout of the test plant and the installation places of the sensors. A switch is used to select the open or closed circuit operation of the plant.*

The maximum mass flow capacity of the test plant is approximately 600 tons per hour. The screen unit was modified in a way that all of the rock material left the screen unit from the conveyor number five.

3.1.1 Belt conveyor

All of the online mass flow sensors used in the experiment were installed in the same belt conveyor number three. The belt conveyor number three is a lifting fixed roller rack conveyor. The belt conveyor is driven with a 10 kW constant speed electric motor. Table 3.1 presents the features of the belt conveyor number three.

Table 3.1. *Properties of the belt conveyor number three*

Feature	Value
Conveyor length (effective)	13.4 m
Conveyor height (lifting)	4.10 m
Conveyor belt velocity	1.45 m/s
Conveyor belt width	1.00 m
Inclination angle of the conveyor	17.4˚

The effective length of the conveyor refers to the length, which the rock material travels on top of the conveyor belt. The conveyor height (lifting) refers to the amount of meters the conveyor system lifts the rock material. The conveyor belt velocity was measured with a tachometer.

3.1.2 Sensor types and quantities

The online mass flow sensors used in the experiment of this work are power transducer, laser profilometer, ultrasonic sensor and strain gauge. The reference mass flow measurement during the experiment is performed with the belt scale. Table 3.2 presents the models and quantities of the sensors used in the measurement setup of this work.

Table 3.2. *The sensor types and quantities used in the measurement setup of this work*

Sensor	Quantity
SEG ZH13 belt scale [24]	1
Endress & Hauser Prosonic T FMU30 ultrasonic sensor [32]	1
Carlo Gavazzi CTP-DIN power transducer [25]	1
SICK Ruler E1200 [28]	1
Kyowa KFG-5-120 strain gauge [33]	3

The sensor models used in this work, had couple of undesired features, which were revealed after the experiments were performed. First of all, SEG ZH13 belt scale was equipped with an intelligent zero setting algorithm, which automatically calibrates the zero mass flow value of the measurement. The automatic calibration algorithm is used to maintain certain accuracy of the belt scale, despite lack of periodic calibration. However, in this work, the belt scale interpreted the small mass flows partly as the tensions of the conveyor belt and generated inaccurate mass flow measurements, while small mass flows were moving on the belt conveyor. Therefore, the results concerning the small mass flow values cannot be analysed.

The second undesired feature of the measurement setup, originated from the low measurement frequency of the ultrasonic sensor. If compared to other industrial ultrasonic sensor models, the measurement frequency of the used model was approximately ten times lower. Higher measurement frequency would have generated more comprehensive measurement data for analysis of the ultrasonic sensor.

3.1.3 Sensor installation

The installation places of the online mass flow sensors are determined by the operating principle of the sensor. While the belt scale and the strain gauges are installed below the conveyor belt (Figures 2.3 and Figure 2.9), the laser profilometer and the ultrasonic sensor are installed above the conveyor belt (Figures 2.5 and Figure 2.8). The installation places of the sensors are presented in Table 3.3 in relation to the length of the belt conveyor. The installation places are declared in relation to the higher end of the conveyor system, which considered the zero point.

Table 3.3. *Installation places of the sensors in the belt conveyor number three*

Sensor type	Installation place
Power transducer	0.00 m
Strain gauges 1,2 and 3	1.95 m
Belt scale	3.13 m
Laser profilometer	4.98 m
Ultrasonic sensor	5.09 m

The power transducer is located in the electrical cabinet of the test plant. However, since it measures the power of the electric motor, which is located at the higher end of the belt conveyor number three, the installation place of the sensor is determined 0.00 meters. All of the strain gauges are installed in the same roller rack of the belt conveyor and therefore the installation place is the same for all of them.

3.1.4 Conveyor belt shape approximation

As presented in the Subsection 2.2.1.3, the shape of the conveyor belt can be approximated with a polynomial equation. The shape of the empty conveyor belt is measured with the laser profilometer and a polynomial equation is fitted to it (Equation 2.16). The polynomial equation describing the profile of the empty conveyor belt is presented in Equation 3.1.

$$f(x) = -1.2 * 10^{-17}x^6 + 3.5 * 10^{-14} * x^5 - 4.0 * 10^{-11} * x^4 + 2.1 * 10^{-8} * x^3 - 4.1 * 10^{-6} * x^2 - 0.00038 * x + 0.19 \quad (3.1)$$

Instead of using the polynomial equation presented in Equation 3.1, the profile of the empty conveyor belt was measured for the ultrasonic sensor with Ruler E1200. This procedure was performed to minimise the errors caused by the conveyor belt shape approximation with a polynomial equation. The error caused by the approximation can be significant, due to the changing conveyor belt profile under the mass of the material. The approximation error of the conveyor belt depends on the conveyor type and size. Therefore, no universal conclusions can be made based on one conveyor profile and experiment. For this reason, the empty conveyor profile measured by the laser profilometer is used for the mass flow estimation model of the ultrasonic sensor.

3.1.5 Bulk density of the rock material

The rock material used in the test plant during the experiment of this work was already pre-crushed. No additional size reduction was performed for the rock material with the crusher unit during the experiment. The bulk density of the rock material, which was used in the experiment, was approximately 1,440 kg/m^3. The bulk density value of the rock material was measured by the operators of the test plant. Figure 3.2 presents the rock material used for mass flow estimation during the experiment of this work.

Figure 3.2. *Rock material used for mass flow measurements during the experiment of this work*

The bulk density value of the rock material is required in the calculations of the mass flow estimates of the laser profilometer and ultrasonic sensor. The average size of the pre-crushed rock material used in this work is in the same order of magnitude than some of the end products of the real aggregate processing plants. This is a valuable feature of the rock material. The optical and ultrasonic measurements are expected to generate the best measurement signals with relatively small sized rock particles moving on the conveyor belt. Small material particles generate a smooth height profile. Therefore, the laserprofilometer doesn't generate blind spots to the height profile. Also, the measurement signal of the ultrasonic sensor is expected to correlate more accurately with the reference mass flow measurement, if the material surface is smooth or even better horizontal.

3.2 Experiment

This subsection presents the experiment performed in this work. Also, the measurement data modifications, delays between the signals and linear regression models are presented. The experiment of this work was performed to acquire measurement data from the online mass flow sensors for data analysis. Only one experiment was carried out in this work. Mass flows up to 400 tons per hour were measured during the experiment. The mass flow fluctuations on the belt conveyor were generated by controlling the feeder unit and the velocities of the conveyors one and two. Figure 3.3 presents the mass flow profile generated with the test plant equipment during the experiment.

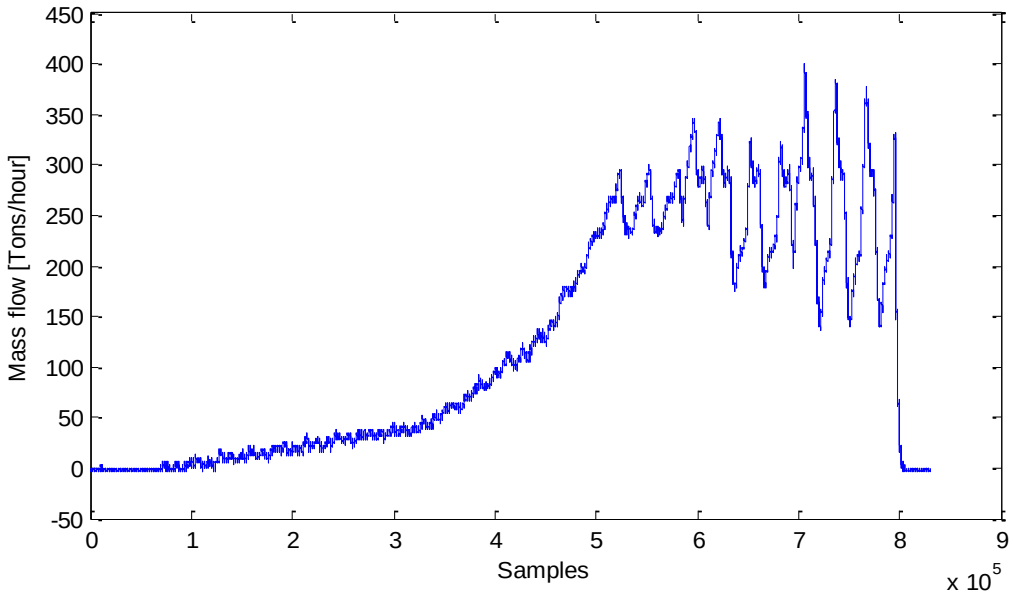

Figure 3.3. *The mass flow profile generated by the test plant equipment during the experiment.*

The duration of the experiment was 27 minutes and 40 seconds. The measurement frequency used during the experiment was 500 Hz. The total amount of 829,696 measurement samples was recorded during the experiment with each online mass flow sen-

sors. The plant was operated as closed-circuit, which enabled large mass flow values to be generated rapidly on the conveyors. The wide scale of the mass flow values measured also makes linearity assessments of the measurement signals possible.

3.2.1 Modification of the measurement data

The measurement data acquired during the experiment of this work consisted of eight measurement channels, including the measurement signals of the online mass flow sensors, belt scale, tachometer and the internal clock of the measurement software. The data-acquisition was performed with DASYLAB measurement hardware and software. The measurement data was stored in ASCII file and modified with MATLAB software.

The inspection and modification of the measurement data was performed to clean the measurement data from outliers, trends and other non-desired features. The first 250,000 and the last 100,000 measurement samples of each measurement signal were considered not suitable for correlation analysis due to the internal calibration features of the belt scale. Also, the degreasing idle power trend was removed from the measurement signal of the power transducer. This was performed for the accuracy analysis of the mass flow estimation model. The modified measurement signals of the power transducer, laser profilometer and ultrasonic sensor were used to create mass flow estimates with the mass flow estimation models presented in Subsection 2.2. The original measurement signals of each online mass flow sensor can found in Appendix A.

3.2.2 Delays

Before the linear regression models for the measurement signals of the online mass flow sensors can be calculated, the signals need to be shifted to same phase with the measurement signal of the belt scale. Therefore, the delays between each online mass flow sensor and the belt scale have to be calculated. A cross correlation of the measurement signals is used to find out the delays between the signals. Table 3.4 presents the delays between each measurement signal of the online mass flow sensor and the reference mass flow measurement signal of the belt scale.

Table 3.4. *The delays between each online mass flow sensor and the reference mass flow measurement of the belt scale*

Sensor	Delay
Power transducer	6.6 s
Ultrasonic sensor	1.3 s
Laser profilometer	2.5 s
Strain gauges	2.0 s

The delays between the measurement signals of the online mass flow sensors and the belt scale consist of two components, which are the measurement delay and the propagation delay. The measurement delays are generated by the internal operations of each

sensor. The propagation delays are generated by the different mounting positions of the sensors in relation to the length of the belt conveyor. The delay of the power transducer is 6.6 seconds, which is caused by the averaging nature of the power measurement. The momentary measurement value of the power transducer represents the average power value over the effective length of the conveyor.

3.2.3 Linear regression models

In order to analyse the correlations and accuracies of the measurement signals of the online mass flow sensors, linear regression models are calculated for each measurement signal. The measurement signal samples between 250,000 and 750,000 are used to calculate the linear regression models. These measurement samples represent a mass flow scale from 30 to 400 tons per hour, according to the belt scale measurements. Table 3.5 presents the linear regression model parameters (Equation 2.20) for each of the measurement signal of the online mass flow sensors.

Table 3.5. *The linear regression parameters for each measurement signal*

Sensor	B	A
Power transducer	63.954	-201.480
Laser profilometer	2436400	11.194
Ultrasonic sensor	11.873	6.200
Strain gauge 1	75.507	62.894
Strain gauge 2	-92.300	61.082
Strain gauge 3	57.892	-24.955

When the correlations of the measurement signals are being analysed in Subsection 4.1, these parameters are used to create the signals for the analysis. The linear regression models were calculated with MATLAB software. The strain gauge number two has a negative slope factor *B* value, which is caused by the mounting locations of the sensor. The strain of the strain gauge number three occurs in opposite direction, compared to the other two strain gauges.

3.3 Error analysis

In order to analyse the reliability of results presented in this work, an error analysis is performed. Multiple factors generate errors and uncertainty to the results, such as the calibration errors of the sensors, parameterisation errors of the mass flow estimation models, measurement errors of the sensors and data-acquisition hardware, and the errors of the linear regression models. This subsection tries to analyse the quantities of these errors and presents a propagation of uncertainty for each measurement signal and result.

3.3.1 Calibration and parameterisation errors

The calibration and parameterisation errors are generated by the inaccuracies of the manual measurements. Manual measurements are required in initial calibration of the sensors and in mass flow estimation model parameterisation. The measurement setup and conveyor were measured with a ruler. The accuracy of these measurements can be estimated to be couple of centimetres depending on the measured parameter. These errors caused by the manual measurements have the most significant effect to the measurement signals of the laser profilometer and the ultrasonic sensor. Initial calibration and parameterisation errors are presented in Table 3.6.

Table 3.6. *The initial calibration and parameterisation errors*

Parameter	Value	Error
Installation height of the laser profilometer	0.86 m	+/− 0.01 m
Installation height of the ultrasonic sensor	1.10 m	+/− 0.01 m
Conveyor width	1.00	+/− 0.01 m
Lifting height of the conveyor	4.1 m	+/− 0.05 m
Dropping height of the conveyor	2.2 m	+/− 0.05 m
Inclination angle of the conveyor	17.4 °	+/− 0.1 °
Coefficient factor	0.74	+/− 0.0074
Bulk density estimate of the rock material	1440 kg/m^3	+/− 72 kg/m^3

The errors generated during the manual measurements of the measurement setup are also generating major errors to the mass flow estimation models. The presented models are very much dependent of the geometrics of the measurement setup.

3.3.2 Measurements errors

The measurement error quantity of the sensor is dependent of the internal accuracy of the sensor as well as the measurement method related errors. The main concern of the measurement error is focusing on the belt scale. The belt scale is used as the reference mass flow measurement in this work. Therefore, the measurement error it generates effects on all of the quantitative results presented in this work. The accuracy of the belt scale used in this work is +/− 1 %, according to the datasheet [24]. However, the real accuracy of the belt scale might be worse, due to the lack of periodic calibration. The velocity error of the tachometer can be ignored, due to the extremely high resolution of the tachometer wheel, which has 40,000 pulses per one revolution.

The laser profilometer has the best accuracy of the sensors used in this work [28]. Also other online mass flow sensors have relatively good accuracies, which are smaller than +/− 1 % [25, 32, 33]. The accuracies of the sensors are presented in Table 3.7.

Table 3.7. *The accuracies of the online mass flow sensors [25, 32, 33]*

Parameter	Accuracy
Power transducer	+/− 0.5 %
Laser profilometer	+/− 0.007 %
Ultrasonic sensor	+/− 0.2 %
Strain gauge (gauge factor error, resistance error, bending of the roller rack)	+/− 0.1 %, +/− 0.3 % and +/− 2 %

Additional errors are generated to the measurement signals, due to the operating principles of the sensors. As presented in Figure 3.4, the height profile of the rock material bed has major effect to the mass flow estimate of the ultrasonic sensor. This error is significant, but the quantity of it is impossible to estimate based on the experiment of this work. Also, the operation principle of the height measurement filtering algorithm of the ultrasonic sensor is unknown. Therefore, it is difficult to analyse, whether the large variations in ultrasonic sensor measurements are actual height values, filtered height values or measurement errors.

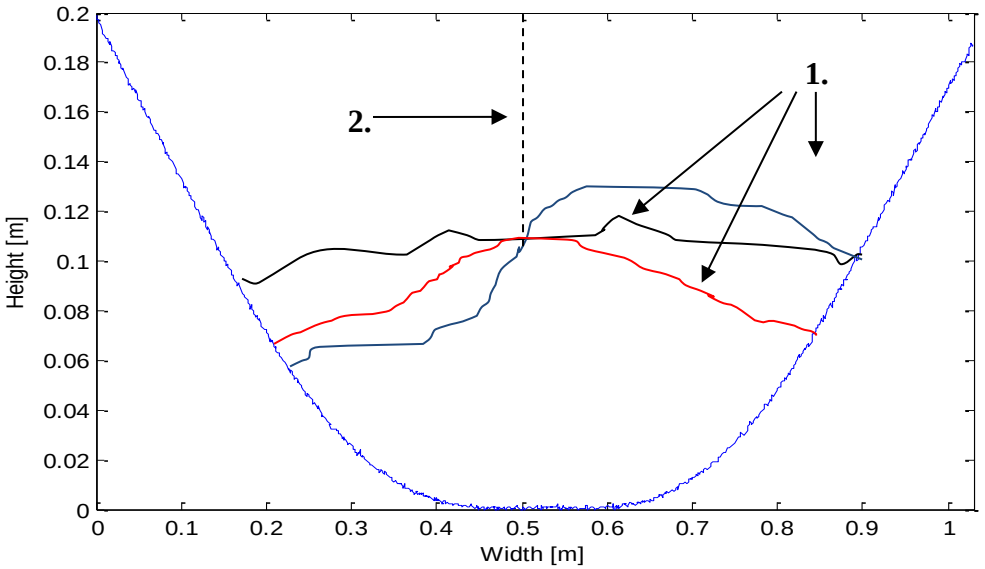

Figure 3.4. *Examples of surface profiles (1). The shape of the height profile has considerable effect to the mass flow estimated using ultrasonic sensor measurement (2).*

The strain gauges have lots of noise added to the measurement signal. This noise is, however, almost uniformly distributed around the zero value. Therefore it doesn't generate major cumulative errors to the analysis. More important source of an error with the strain gauges is the non-desired bending of the roller rack against the measurement direction of the strain gauges. This bending is caused by the moving loaded conveyor belt.

Figure 3.5 presents how the forces are affecting the strain gauge element. The amount of this error is estimated to be +/− 2 %. As presented in Figures 5 and 6 in the Appendix A, the strain gauges number one and two are most affected by this phenomenon. The strain gauge number three was almost immune to this phenomenon, due to optimal installation place of the sensor.

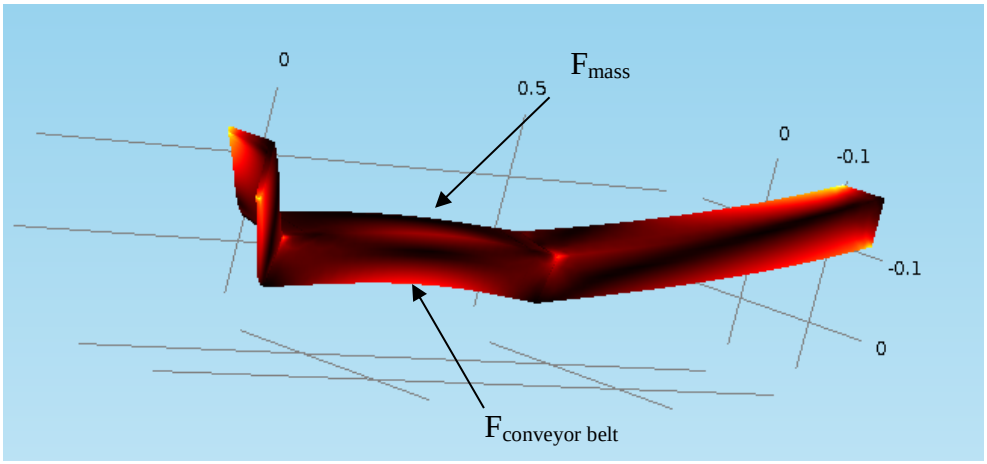

Figure 3.5. *The conveyor roller rack and the forces affecting it. The strain gauge is supposed to measure the strains caused by the mass on the conveyor (F_{mass}=mg). However, the force generated by the moving conveyor full of rock material $F_{conveyor\ belt}$ causes error to the measurement signal by bending the roller rack.*

The power transducer and the laser profilometer don't have significant errors generated due to the operation principles of the sensors. On the contrary, the power transducer has one major benefit against the other online mass flow sensors. Due to the operating principle of the power measurement, the measurement value has strong filtering over the effective length of the conveyor. This feature is expected to decreases the momentary measurement errors of the mass flow with the belt scale.

3.3.3 Data-acquisition and linear regression errors

The errors caused by the data-acquisition hardware and linear regression are estimated to be very small. Low signal levels cause quantization error to the measurement signals of the strain gauges. However, this error is filtered of due to the high measurement frequency (500 Hz) and noise in the measurement signal. Since the errors caused by the data acquisition system cannot be reliably estimated, they are left out of the uncertainty calculations of the measurements. The errors caused by the linear regression method are in relation to the calculation accuracy of the software used for linear parameter estimation. This error is considered to be very small due to the automatic nature of the linear regression method applied to the measurement signals. If the linear regression parameters were estimated manually, then this error would also be included in the uncertainty calculations.

3.3.4 Propagation of uncertainty

The uncertainty of the measurement signal of the online mass flow sensor is a combination of all the error sources affecting it. The uncertainty of the mass flow estimate Δf_{est} can be calculated by the propagation of uncertainty presented in Equation 3.2. [40]

$$\Delta f_{est} = \Delta f(x_1, x_2, \dots, x_n, \Delta x_1, \Delta x_2, \dots, \Delta x_n) = \sqrt{\sum_{i=1}^{n} \left(\frac{\partial f}{\partial x_i} \Delta x_1\right)^2} \tag{3.2}$$

Where x_i is the variable that affects the uncertainty of the mass flow estimate, Δx_i is the estimated error of the individual variable [40]. The errors, which are used to calculate the uncertainty values for each the mass flow estimates, are presented in Tables 3.6 and 3.7. If the error of the belt scale is also included in the uncertainties, Equation 3.3 is used to calculate the cumulative of uncertainties $\Delta f_{cumulative}$ of the mass flow estimates [40].

$$\Delta f_{cumulative} = \Delta f(x_1, x_2, \dots, x_n) = \sqrt{\sum_{i=1}^{n} (\partial x_i)^2} \tag{3.3}$$

Equations 3.4 to 3.7 present the uncertainties for each mass flow estimate (PT = power transducer, LP = laser profilometer, US = ultrasonic sensor and SG = strain gauge). The estimated errors are calculated from the maximum values of the measurement signals. This way the calculated values are valid in throughout the whole mass flow scale.

$$\Delta f_{est\_PT} = \sqrt{\left(\frac{45\ W}{9000\ W}\right)^2 + \left(\frac{0.0074\ m}{0.74\ m}\right)^2 + \left(\frac{0.05\ m}{4.1\ m}\right)^2 + \left(\frac{0.05\ m}{2.2\ m}\right)^2 + \left(\frac{0.1^\circ}{17.4^\circ}\right)^2}$$

$$\Delta f_{est\_PT} = 2.87\ \% \tag{3.4}$$

$$\Delta f_{est\_LP} = \sqrt{\left(\frac{72\ kg/m^3}{1440\ kg/m^3}\right)^2 + \left(\frac{0.01\ m}{0.86\ m}\right)^2 + \left(\frac{0.00004\ m}{0.105\ m}\right)^2 + \left(\frac{0.01\ m}{1.0\ m}\right)^2} = 5.23\ \% \tag{3.5}$$

$$\Delta f_{est\_US} = \sqrt{\left(\frac{72\ kg/m^3}{1440\ kg/m^3}\right)^2 + \left(\frac{0.01\ m}{1.1\ m}\right)^2 + \left(\frac{0.00021\ m}{0.105\ m}\right)^2 + \left(\frac{0.01\ m}{1.0\ m}\right)^2} = 5.18\ \% \tag{3.6}$$

$$\Delta f_{est\_SG} = \sqrt{\left(\frac{0.0207}{2.07}\right)^2 + \left(\frac{0.36\ \Omega}{120\ \Omega}\right)^2 + \left(\frac{2.4\ \Omega}{120\ \Omega}\right)^2} = 2.26\ \% \tag{3.7}$$

Table 3.8 presents the uncertainties for each measurement signal of the online mass flow sensors. The uncertainties of the linear regression models are derived from the accuracies of individual sensors, which are presented in Table 3.7. Individual uncertainties are calculated for the linear regression and the mass flow estimation models. The last column indicates the cumulative uncertainty of the mass flow estimates, if the belt scale error is added to the uncertainties of the measurements (Equation 3.3).

Table 3.8. *The uncertainties calculated for each of the measurement signal*

Sensor	Uncertainties of the mass flow estimates Δf_{est} (mass flow model, linear regression)	Cumulative uncertainties of the mass flow estimates $\Delta f_{cumulative}$ (mass flow model, linear regression)
Power transducer	+/− 2.87 %, +/− 0.5 %	+/− 3.04 %, +/− 1.12 %
Laser profilometer	+/− 5.23 %, +/− 0.007 %	+/− 5.32 %, +/− 1.00 %
Ultrasonic sensor	+/− 5.18 %, +/−0.2 %	+/− 5.28 %, +/− 1.02 %
Strain gauge	− , +/− 2.26 %	− , +/− 2.47 %

Based on the uncertainties presented in Table 3.8 the reliably of the results of this work can be evaluated appropriately. The real uncertainties of the measurement signals might be higher, due to additional inaccuracies of the measurement hardware. However, since these calculations cannot be performed reliably, the cumulative uncertainty values presented in Table 3.8 are used in this work.

4. RESULTS

This chapter presents the results of this work and answers each of the 3 research questions formulated for this work. The subsections of this chapter are organised according to the research questions of this work. The first two subsections deal with the quantitative issues, while the third subsection is concentrated on the qualitative issues of the online mass flow sensors.

4.1 Correlation of measurement signals

Based on the linear regression models presented in Subsection 3.2.3 and the reference mass flow measurement signal of the belt scale, a Goodness of Fit analysis is performed with the methods described in Subsection 2.4. Each measurement signals of the online mass flow sensors, was shifted to same phase with belt scale. Then the linear regression method was applied to the measurement signals. Since, the linear regression method generates the best possible (two parameter) linear models for the measurement signals, they can be compared to the mass flow measurement signal of the belt scale.

The RMSE method analyses the rooted average squared errors, while the R-squared method evaluates how well each linear regression models correlates with the belt scale measurement. Table 4.1 presents the results of the RMSE and R-squared methods. The same measurement data, which was used in the calculation of the linear regression models, was used in the Goodness of Fit analysis (measurement samples: 250,000-750,000).

Table 4.1. *Results of RMSE and R-squared methods for each measurement signal*

Sensor	RMSE	R-squared
Power transducer	12.8 +/− 0.14 tons	0.984 +/− 0.011
Laser profilometer	16.0 +/− 0.16 tons	0.975 +/− 0.001
Ultrasonic sensor	19.9 +/− 0.20 tons	0.961 +/− 0.009
Strain gauge 1	32.9 +/− 0.81 tons	0.894 +/− 0.022
Strain gauge 2	37.7 +/− 0.93 tons	0.861 +/− 0.021
Strain gauge 3	19.1 +/− 0.47 tons	0.964 +/− 0.023

Based on the results presented in Table 4.1, the measurement signal of the power transducer has the best correlation values compared to the reference mass flow measurement of the belt scale. The RMSE and R-squared values of 12.8 tons and 0.984 indicate very good mass flow estimation capabilities of the power transducer. The excellent results of the power transducer are due to the mass related operation principle of the

sensor. Previous research in the field of mass flow measurements with the power transducer has also presented very good accuracy against the belt scale [7].

The measurement signal generated by the laser profilometer has also very good RMSE value of 16.0 tons and R-squared value of 0.975. Good correlation and accuracy results could be expected, due to the operating principle of the laser profilometer. The laser profilometer can measure the momentary volume flow changes with very good accuracy and measurement frequencies of up to 10,000 profiles in a second.

The measurement signal of the ultrasonic sensor was proven surprisingly well correlated with the reference measurement of the belt scale. RMSE value of 19.9 tons and R-squared value of 0.961 indicate that the measurement signal of the ultrasonic sensor is very well correlated throughout the whole mass flow scale. This is unexpected since the height measurement is not linear compared to the volume flow, and therefore to the mass flow. The measurement signal of the ultrasonic sensor included large momentary measurement errors. However, the RMSE value is not significantly higher compared to the laser profilometer. The good linear correlation might be due to the wide conveyor belt used in the experiment, which generates fairly low and smooth surface profile for the rock material.

Strain gauges have large variation in both RMSE and R-squared values. The strain gauge number three has almost equal values of 19.1 tons and 0.964 compared to the power transducer. The strain gauges numbers one and two have by far the poorest results of all mass flow sensors. The operating principle of the strain gauge is mass related, which explains the good correlation values. However, the strain gauge measurement is prone to additional forces, which generate strains to the measured object. The results indicate that the installation place of the strain gauge (Figure 2.15) has significant effect to the mass flow estimation capabilities of the sensor. If properly installed, the measurement signal of the strain gauge is well correlated with the reference mass flow measurement of the belt scale.

Figure 4.1 presents a small section of the mass flow data. The effects of the operating principles of the sensor to the mass flow estimate are demonstrated. The mass flow estimate of the power transducer is very smooth due to the averaging nature of the power measurement. The mass flow estimate of the laser profilometer demonstrates the accurate momentary mass flow measurement capabilities of the sensor. The large momentary measurement errors of the ultrasonic sensor are caused by the operating principle of the sensor. The mass flow estimate of the strain gauge correlates very well with the reference measurement, due to the similar operating principle of the sensors. All of the signals have been filtered with a moving average filter of 500 samples for better visualisation. The complete linear regression model estimates of the measurement signals and the reference measurement of the belt scale can be found in Appendix B of this work. The figures presented in Appendix B indicate the linearity of the measurement signals. Good linearity of the measurement signal is presented for power transducer, laser profilometer, ultrasonic sensor and strain gauge number three. Strain gauges number two and three are affected by the undesired force of the conveyor belt. Therefore, the linear

regression parameters are calculated based on the inaccurate measurement signal, which leads to poor linear behaviour with the reference mass flow measurement of the belt scale.

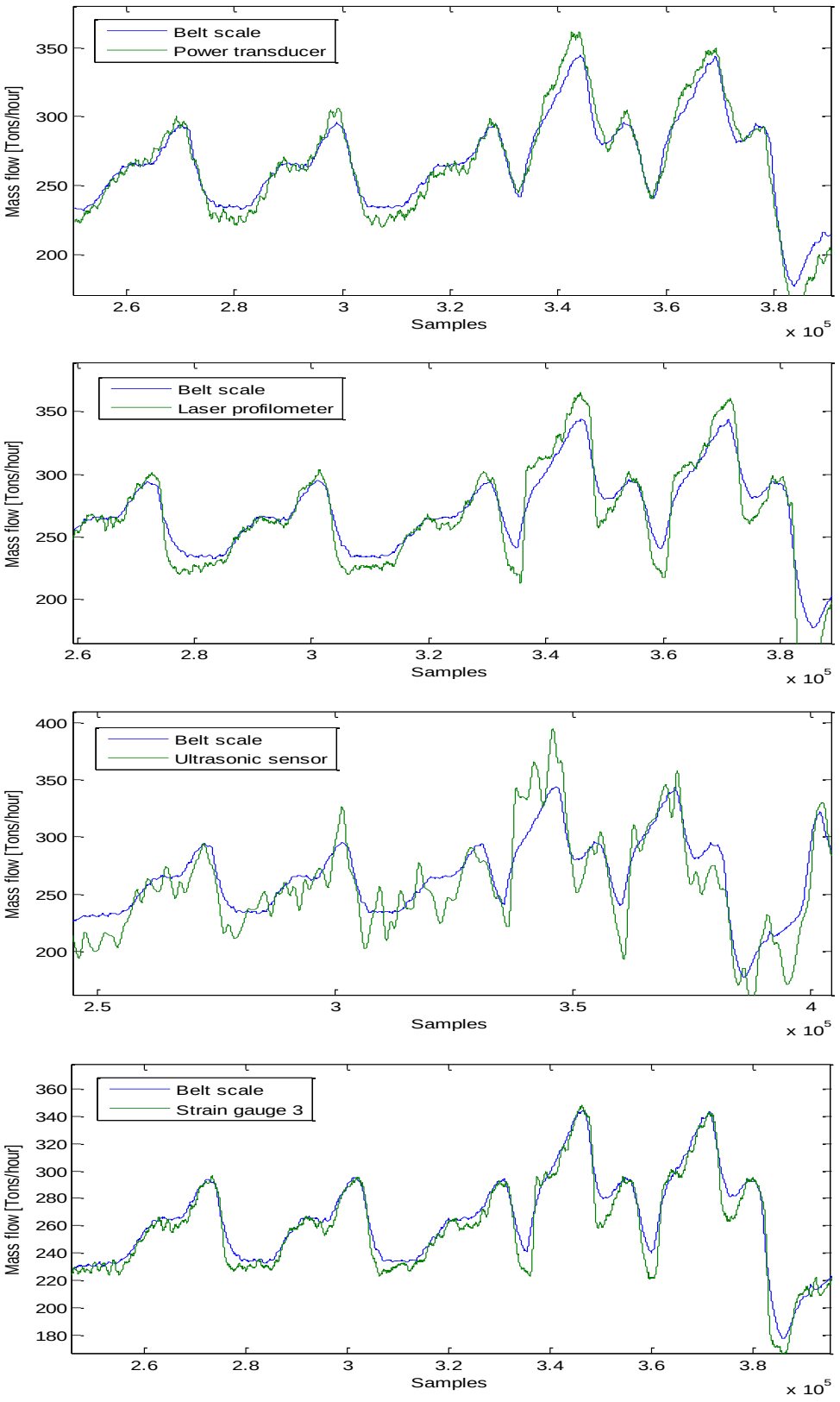

Figure 4.1. *The linear regression model estimates of the online mass flow sensors and the reference mass flow measurement of the belt scale.*

In addition to the RMSE and R-squared values the measurement signals can be analysed by the distribution of residuals presented by histograms. Histogram presents the residuals between the linear regression models and the belt scale measurement as error distribution. Histogram consists of equally spaced intervals, the height of which indicates the amount of observations within the corresponding pin. The total area of the histogram equals the total amount of error. The shape of the histogram indicates how accurately the linear regression model fits the reference mass flow measurement. A narrow shape of the histogram close to the zero value indicates good fit while a broader histogram stands for increased number of bigger residual values. A non-zero centralised histogram indicates that the measurement signal of the mass flow sensor has a systematic error introduced in the signal. Figure 4.2 present a histograms calculated based on the residuals of the linear regression model estimate of the power transducer and the mass flow measurement of the belt scale. [40]

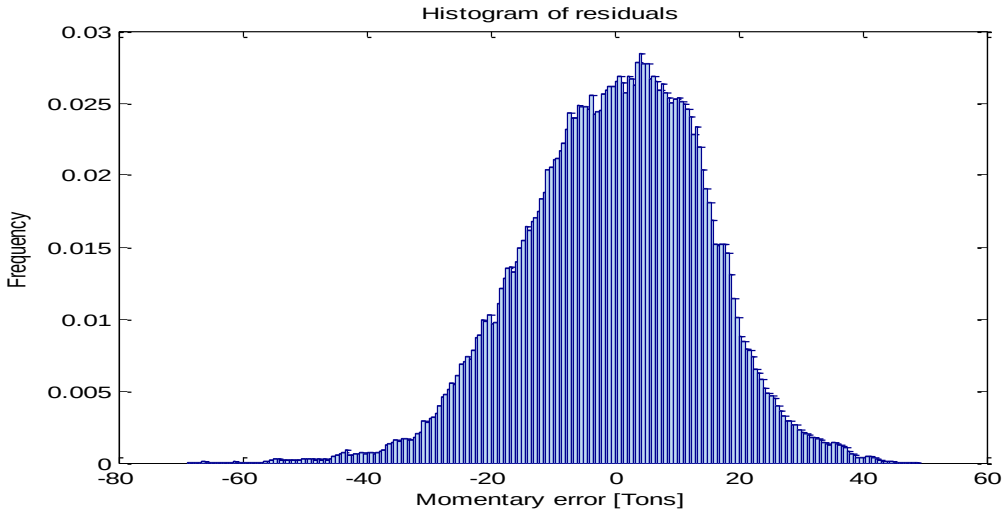

Figure 4.2. *The distribution of residuals between the measurement signals of the power transducer and the belt scale.*

As presented in Figures 4.2 the residual distribution of the power transducer is concentrated around the zero and the shape of the distribution is relatively smooth, which indicates good correlation with the reference mass flow measurement which was also indicated by Table 4.1. Histograms for all of the linear regression models can be found in Appendix C of this work. The reason for smooth residual distribution of the power transducer is the averaging nature of the measurement. The mass flow measurement of the power transducer is an average value over the effective length of the conveyor belt. The more uneven distribution of residual of the ultrasonic sensor might be due to the non-linear correlation between the height measurement and the mass flow measurement. The residual histogram of the ultrasonic sensor is also wider due to the significant amount of large momentary measurement errors. The histogram of the laser profilometer indicates that most of the measurement samples have small residuals values, however, large residual values are also presented. The large residual values are most likely caused by the accurate measurement operation of the laser profilometer and the filtered

signal of the belt scale. The residual histograms of the strain gauges indicate good correlation with the belt scale presented by small residual values and narrow shape of the histogram.

Based on the results presented in this subsection, it can be stated that all of the measurement signals of the online mass flow sensors correlate well with the reference mass flow measurement of the belt scale. However, this requires properly performed installation of the sensors. Poorly chosen installation place of the mass flow sensor has dramatic effect to the correlation capabilities of the measurement with the reference mass flow measurement, which can be noticed from the results presented for the strain gauges numbers two and three. The feature can also be noticed from the figures presented in Appendix B. Also the results of the ultrasonic sensor have to be addressed critically, since the conveyor type and size, measurement setup and the height scale of the rock material profile are not universal. The experiment of this work represents only one type of measurement situation, conveyor belt and height scales of the measured surface. The results presented for the power transducer, laser profilometer and strain gauges can be considered more reliable due to the more robust natures of operations principles of the sensors.

4.2 Accuracy of the mass flow estimation models

This subsection analyses the accuracy of the mass flow estimation models presented in Subsection 2.2. The accuracy of the model is determined by the cumulative error between the mass flow estimate generated by the model and the reference mass flow measurement of the belt scale. Mass flow estimates are generated by the power transducer, laser profilometer and ultrasonic sensor. The total cumulative mass flow value measured by the belt scale during the experiment was 56,147 kg. Table 4.2 presents the cumulative mass flow estimates and errors of each sensor.

Table 4.2. *The cumulative mass flow values and the cumulative errors generated by the online mass flow sensors*

Sensor	Cumulative mass flow value	Cumulative error
Power transducer	56,600 +/- 1,700 kg	0.91 +/- 0.03 %
Laser profilometer	56,600 +/- 3,000 kg	0.88 +/- 0.05 %
Ultrasonic sensor	58,600 +/- 3,000 kg	4.45 +/- 0.24 %

As presented in Table 4.2, the mass flow estimation models of the power transducer and laser profilometer were proven very accurate with the cumulative error values of 0.91 % and 0.88 %. The mass flow estimation model of the ultrasonic sensor was proven relatively inaccurate with the cumulative error value of 4.45 %. The unstable and variable surface profile of the rock material bed is expected to cause most of the inaccuracy (Figure 3.4).

Based on the results presented in this subsection, it can be stated that the mass flow estimation models of the power transducer and laser profilometer are very accurate, with errors smaller than 1 %. The mass flow estimation model presented for the ultrasonic sensor was proven relatively inaccurate. It indicated the accuracy of about 5 % compared with the belt scale. In order to analyse the accuracies of the mass flow estimation model more comprehensively, multiple experiments are required for statistical analysis. The answers presented for the research question number two, should be evaluated critically. Multiple error sources listed in Subsection 3.3, increased the uncertainties of the results. Also, the lack of multiple experiments and the unknown real accuracy of the belt scale are reducing the reliability of the results.

4.3 Features of the online mass flow sensors

This subsection presents answers for the research question number three, which is concerning the qualitative features of the online mass flow sensors. Both financial and operational features of the online mass flow sensors are presented in this subsection. The evaluation matrix presents answers for the research question number three, but doesn't include all possible factors that need to be addressed. Utilisation of the online mass flow sensors in a real life mineral processing plant requires understanding of multiple features of the sensors. Table 4.3 presents some of the important factors, which can be specified for each online mass flow sensor.

Table 4.3. *Operational and financial factors that need to be considered, if the online mass flow sensors are used in a real life mineral processing plant.*

Feature	Power transducer	Strain gauge	Laser profilometer	Ultrasonic sensor	Belt scale
General					
Price	500 €	500 €	15 k€	500 €	5-10 k€
Accuracy (sensor)	0.5 %	1.0 % (1) 0.5% (2)	< 1 mm (3)	0.5%	1 %
Measurement frequency	> 1,000 Hz	(4)	10,000 Hz	0.5-10.0 Hz	1.0 Hz
Data transfer	mA	mA	Ethernet	mA	mA
Unit of measurement	Power	strain	height vector	height	mass flow
Measurement type	average over length (5)	average over length (6)	exact	exact	average over length (6)
Filtering due to the nature of the measurement method	strong	moderate	no	no	moderate
Unknown parameters	Pidle, n	-	bulk density	bulk density	-
Temperature dependency	yes	yes	no	yes	yes
Maintenance demand	no	no	yes	yes	yes
Weather protection demand	yes	yes	yes	yes	yes
Additional equipment required	current sensor	(7)	computer	no	no
Requirement for lifting conveyor	yes	no	no	no	no
Need for filtering	yes	yes	no	yes	no
Installation place	electrical cabinet	conveyor structures	above conveyor	above conveyor	below conveyor
Ability to measure small mass flows	good	good	good	moderate	moderate
Reference mass flow measurement required for calibration	yes	yes	yes	yes	no
Based on the results of this work					
Noise	moderate	large	small	moderate	small
Zero level drift	yes	yes	no (8)	no (8)	no

(1) Gauge factor error (2) Gauge resistance error (3) Resolution of the distance measurement (4) Depends on the operational amplifier and the data-acquisition system (5) Average over the effective length of the belt conveyor (6) Average over the length between the neighbouring roller racks of sensor (7) An operational amplifier and a Wheatstone bridge if it is not integrated to the amplifier unit (8) If installed properly on top of the roller rack, no calibration required

The belt scale is an accurate online mass flow sensor, if it is properly installed and calibrated. It can be installed to various types of conveyor structures. The installation place of the belt scale is below the conveyor belt. The belt scale measures mass flows directly, and therefore, no reference measurement is required for calibration. The output of the belt scale is usually smooth, due to the operating principle of the sensor and internal filtering algorithms. The zero level variations of the mass flow signal are usually compensated automatically in the belt scale. Despite the good mass flow measurement capabilities of the belt scale, the high unit price of the sensor prevents the installation of multiple belt scales into a single mineral processing plant. The unit price of a single belt scale varies depending on the measurement roller racks and accuracy of the belt scale. The unit prices of the belt scales are between 5,000 to 10,000 Euros.

The power transducer is a very good sensor for mass flow estimation in belt conveyors. The power transducer measures the power consumed in the electric motor driving the belt conveyor. The accurate mass flow estimation with the power transducer requires a lifting belt conveyor. The sensor can be installed in various locations, such as electrical cabinets. The correlation of the power measurement signal and the mass flow is dependent of multiple factors, which cannot be accurately measured online. The coefficient factor of the belt conveyor has major impact to the accuracy of the mass flow estimate. This factor is not constant, but depends on multiple variables, such as frictions of the belt conveyor, ambient temperature and coefficient factor of the electric motor. Also, the idle power drift causes inaccuracy to the mass flow estimates generated by the power transducer measurement. The unit price of the power transducer is approximately 500 Euros.

The laser profilometer has very good mass flow estimation capabilities, if properly installed, calibrated, maintained and operated by educated personal. Also, a relatively constant bulk density value of the measured material is required, in order to generate accurate online mass flow estimates. All of these demands are usually hard to meet at the same time, which makes the laser profilometer accurate but non-optimal sensor for online mass flow estimation in mineral processing applications. The installation place of the laser profilometer is above the belt conveyor. The high unit price of approximately 15,000 Euros decreases the desirability of the laser profilometer as the main mass flow sensor at the mineral processing plants. However, the good internal accuracy of the sensor and the exact operating principle result in great mass flow estimation accuracy. If compared against the other online mass flow sensors, the laser profilometer has one major benefit. It can be used to generate size distribution estimates for the material from the conveyor [15]. This feature might increase the desirability of the laser profilometer in the future. The size distribution estimate of the rock material can be used to online control the rock crusher units.

The ultrasonic sensor provides a simple and affordable online mass flow measurement from belt conveyors. The ultrasonic distance measurement is already used in the mineral processing applications and proven feasible in the harsh operating environment of the industry. A relatively constant bulk density value of the measured material is

required, in order to generate accurate online mass flow estimates. The installation place of the ultrasonic sensor is above the conveyor belt. The zero level change of the distance measurement can generate errors to the measurement signal correlation with the mass flow. Also, large ambient temperature variations may cause significant errors to the distance measurement. The momentary values of the distance measurement don't necessarily correlate well with mass flow values. However, the experiment of this work indicated that the average height of the rock material bed has good correlation with the mass flow. The low unit price of approximately 500 Euros and the low maintenance requirements of the ultrasonic sensor, make it well suited as online mass flow sensor in mineral processing applications.

The strain gauges are the most common mass flow sensors type used in commercial belt scales. This work analysed how well the strain gauge element can estimate mass flows, when installed in the belt conveyor structures. The installation place of the strain gauge was proven extremely important. Good linear correlation of the strain measurement and mass flow was noticed only with one of the three strain gauges. The measurement signal of the strain gauge has considerable amount of noise, compared to other measurement signals of the online mass flow sensors. The strain gauge measurement system costs approximately 500 Euros. The strain gauge has great potential to be used as an affordable, simple and durable online mass flow sensor in mineral processing applications in the future.

As presented above, various factors need to be considered, if the online mass flow sensors are utilised in mass flow estimation in mineral processing applications. The optimal sensor, or sensor combination for each mineral processing plant is determined by the financial and operational requirements and restrictions set for the measurement system. Also, other factors, such as availability of a reference mass flow measurement, belt conveyor specifications, data transfer methods and accuracy requirements play significant role in the selection of the optimal online mass flow measurement. Ignoring the consideration of the factors presented in Table 4.3 may lead to poor measurement accuracy and nonlinear behaviour of the mass flow measurement.

5 DISCUSSION

This chapter includes a discussion part of this work, which compares the results against the previous academic and company financed research. This chapter also explains why this work and its results are relevant to the mineral processing industry.

The main goals of this work are formulated as three research questions. The research question number one is focused on analysing the correlations of the measurement signals of the presented online mass flow sensors with the reference mass flow measurement of the belt scale. The research question number two is focused on analysing how accurate the presented mass flow estimation models are. The research question number three is dealing with the features, strengths and weaknesses of the online mass flow sensors. The results presented for these questions in Chapter 4, are now compared against the previous research in the field of mass flow measurements.

Power transducers have been previously studied as cost-effective mass flow sensors in aggregate production plants [7]. Research with this sensor type has given promising results. The results, generated by multiple real life aggregate production plant experiments, indicate that the accuracy of the power transducer measurements compared to the traditional belt scale is approximately +/− 2 % [7]. An accuracy value, which can be considered very good within the aggregate production industry. The results presented in this work also indicate similar accuracy values for the mass flow estimation model of the power transducer. This work also analysed the correlation of the measurement signals of the power transducer and the belt scale. The results of this analysis indicated good correlation of the two signals. Even though, the mass flow estimation with the power transducer has multiple factors that need to be considered, it has great potential to be used in the mineral processing applications throughout the industry. The mass flow estimation model presented by Hulthén, didn't utilise any active idle power compensation algorithm, but still indicated a very good performance of the mass flow measurement [7]. These results indicate that the error generated by idle power drift would not be significant during long measurement periods. In this work the idle power drift however required compensation due to the short experiment duration.

Optical measurement methods, such as machine vision-based systems are widely researched in mining and mineral processing. They have proven suitable in some parts of the processes. Multiple camera technologies, such as 2D, 3D and laser profilometer have been researched as a way of monitoring material volume flows and particle size distributions [12, 13, 14, 15]. Machine vision is also widely used for general monitoring of the mineral processing plants. The results of this work indicate that the correlation between the measurement signal of the laser profilometer and the belt scale is very good. Also, the mass flow estimation model presented in this work was proven very

accurate. Despite the potential volume and size distribution measurement methods, presented by the previous academic research and this work, the optical measurement systems have multiple deficiencies that prevent the wider installation of these systems in minerals processing applications. In addition to the high unit price, the most fundamental problem with the optical measurement systems is that they can only measure the volume flow or size distribution of the material moving on the conveyor. In order to obtain estimate for the material mass flow, the bulk density of the material has to be measured. Until the bulk density estimation of the material can be automated with sufficient accuracy, the optical measurement methods will most likely to be used only for volume flow and size distribution estimation.

Ultrasonic sensors are previously researched as volume flow sensors in multiple applications, such as conveyors and silos [16]. In this work, the measurement signals of the ultrasonic sensor and the belt scale were analysed, and good correlation of the two signals was detected. The mass flow estimation model of the ultrasonic sensor was proven relatively inaccurate. When properly installed, calibrated and operated, the affordable ultrasonic sensor has great potential to be used as a mass flow sensor in the future. However, the same fundamental problem concerning the bulk density estimation of the material has to be resolved, before the full potential of the ultrasonic sensor can be utilised in the mass flow estimation.

Strain gauges are the most fundamental sensor type used for mass flow measurements [18]. Basically, all of the commercial belt scale systems utilise strain gauges. However, belt scale systems are too expensive to be used for plant wide online mass flow monitoring in mineral processing applications. For this reason, this work analysed the correlation of the measurement signals of the belt scale and the strain gauges installed in the belt conveyor roller racks. By applying the linear regression method to the strain gauge measurement signal, a good correlation with the belt scale measurement was detected. This work analysed only one potential installation place of the strain gauges. The strain gauge has great potential in mass flow estimation in mineral processing plants, due to the simple and durable operating principle and the low unit price of the sensor. More research is however required with this method, before it can compete against the high accuracy, auto-calibrated commercial belt scale systems.

In order to achieve similar results as presented in Tables 4.1 and 4.2, the utilisation of the presented online mass flow sensors requires understanding about the features and error sources of each measurement signal. Multiple procedures concerning installation, calibration, filtering and data processing have to be considered and properly performed in order to achieve good correlation of signals. Even better correlation of the signals might be achieved by more complex linear regression models. Especially, with the presented mass flow estimation models the parameterisation of the model equations need to be performed accurately.

As a summary of the results of this work, it could be said that, all measurement signals of the online mass flow sensors correlate well with the reference mass flow measurement of the belt scale. This result demonstrates the potential online mass flow

estimation capabilities of the sensors. Also, the mass flow estimation models for the power transducer and laser profilometer were proven accurate. However, the presented online mass flow sensors require a reference mass flow measurement, in order to be calibrated accurately. The reference mass flow measurements could be, for example, a belt scale. Also, a wheel loader scale could be used to generate the reference mass flow measurement. Even the truck scales could be used for long period statistical calibration of the online mass flow sensors. Methods for the calibration don't yet exist, which delays the implementation of the online mass flow sensors presented in this work. If methods for the sensor calibration are developed, the online mass flow sensors provide accurate and cost-effective mass flow measurements from the mineral processing plants. The unit prices of the power transducer, ultrasonic sensor and strain gauge are in order of tenth of the traditional belt scale. The low unit price of the sensors allows monitoring of the whole mineral processing plant cost-effectively. Provided that the features and restriction of each sensor type are addressed properly and that the reference mass flow measurement is available for calibration.

6 CONCLUSIONS

This chapter presents the conclusion that can be made based on the results of this work. Only one experiment was performed in this work. Therefore, the scientific base of the conclusions should be evaluated with proper perspective. Future research proposals are also presented in the field of online mass flow estimation in mineral processing applications.

6.1 Conclusions

The demand of more comprehensive online mass flow measurements in mineral processing plants is expected to increase in the future. Ever hardening competition, increasing energy prices, tightening environmental safety requirements and other factors strain the profits of the companies, which are working in the mineral processing industry. In order to stay profitable in the future, companies need to make investments to new technology, such as automated control and optimization systems. These systems are designed to optimize the operation of the mineral processing plant. However, they cannot operate efficiently without online mass flow measurements from the plant.

The most common online mass flow sensor used in the mineral processing is the traditional belt scale. Due to the high unit price of the belt scale, it cannot be used for plant wide online mass flow monitoring in mineral processing. Offline mass flow sensors, such as the wheel loader scales and the truck scales cannot be used for online mass flow measurements either. The problem concerning the online mass flow measurements is obvious. In order to implement new automated control and process optimisation systems to the mineral processing plants, alternative online mass flow measurement methods need to be developed.

The mass flow measurement equipment is usually considered too expensive to be implemented to the mineral processing applications, such as aggregate production processes. The benefits of the online mass flow measurements have also been considered controversial. The operating costs of the mineral processing plants are significant, due to large energy consumption and spear parts usage. Therefore, even minor improvements in the process control could produce major financial benefits for the companies. The research performed in the field of process modelling indicates that major improvements in the processes could be achieved with the usage of more advanced process control and optimisation systems [7, 8, 9, 10, 11].

The results of this work presented that, alternative online mass flow sensors and estimation models can be found to replace or work side by side with the traditional online mass flow sensors. However, one major issue still stands in the way of implementation of these sensors, the calibration of the sensors. A reference mass flow measurements

need to be available for calibration of the sensors. Belt scales, wheel loader scales and truck scales could be used to create the reference mass flow measurement.

More comprehensive monitoring of the mass flows provides valuable information for the companies building and designing the mineral processing equipment. Product development departments can utilize the online mass flow measurements to design new equipment and control structures. If the mass flows are measured after the screen unit, an estimate for the rock material size distribution can be calculated. The size distribution estimate can be used for automated control of the crusher units. The more comprehensive monitoring of mass flows enables development of dynamic simulation models for the mineral processing plants and equipment. The monitoring of multiple material streams also generates fault diagnostics capabilities for the mineral processing plants. The benefits gained by the online mass flow estimation could be significant in terms of development and implementation of automated process control and optimisation systems. These valuable measurements should not be over looked anymore by the mineral processing plants. Based on the results of this work, the companies working in the industry are suggested to start invest more to the development of the online mass flow sensors and measurement systems.

Before the fully automated monitoring and optimisation systems are available on the markets, the mass flow sensors presented in this work can be utilised also in the manual control of the mineral processing plants. The online mass flow measurements and statistics of the production volumes can be used to estimate optimal operational parameters of the equipment. Also, production scheduling can be performed based on the online mass flow measurements of the end products.

6.2 Future work

This subsection presents future research proposals for the mass flow estimation in mineral production applications. The features and phenomena of the online mass flow sensors, which came up during this work, generated multiple potential future research topics. Originating from the results of this work, the most important issue to be resolved is the calibration of the online mass flow sensors.

Additional research is required with quantitative issues, such as the measurement signal correlations, data filtering and synchronising, and mass flow estimation models. More measurement data should be acquired with the online mass flow sensors for more comprehensive statistical analysis. Also, qualitative issues concerning the operational performance of the online mass flow sensors needs further studying. Mass flow estimation, with the presented online mass flow sensors, requires solutions for optimal and rugged installation of the sensors. Especially, the strain gauge installation requires further research. The future research proposals, which originated from the results and conclusion of this work, are presented in the two categories, analytical and operational.

- **Analytical**
  - Calibration of the sensors (highest priority)
  - Online filtering of the mass flow measurement signals
  - Automatic data synchronising (multiple mass flow measurements to same phase)
  - Utilisation of multiple mass flow measurements in dynamic modelling of the mineral processing plant
  - More complex linear regression model fitting to measurement signals of the online mass flow sensors
  - FEM software utilisation to find the optimal installation place for strain gauges

- **Operational**
  - Rugged and low maintenance installation methods for the online mass flow sensors
  - Testing of alternative installation locations for the strain gauges
  - Implementation method for choosing the optimal sensor combination to mineral processing plant layout
  - Mass flow estimation with mobile aggregate production plants
  - Sensor fusion in mass flow estimation

Further research is also required concerning methods evaluating and indicating the financial benefits, which could be gained by more advanced online mass flow measurements. Mineral processing plants are expected to be more willing to invest in the mass flow measurement systems, if the financial benefits can be estimated and presented.

REFERENCES

[1] European Aggregates Association. (2008). What are aggregates? [Online] Available: http://www.uepg.eu/what-are-aggregates [20.8.2012]

[2] European Aggregates Association. (2008). Current trends for the European Aggregates Sector. [Online] Available: http://www.uepg.eu/statistics/current-trends [20.8.2012]

[3] Adel, G., Kojovic, T. and Thornton, D. (2006). Mine-to-Mill Optimization of Aggregate Production – Final Report. Queensland, Australia. Julius Krutschnitt Mineral Research Centre.

[4] Houtman, C. (2008). Aggregates production technology. [Online] Available: http://www.eoearth.org/article/Aggregates_production_technology [6.9.2012]

[5] Rudus Oy. (2012). Kiviainehinnasto, Tampere-Vaasa. [Online] Available: http://www.rudus.fi/aineistot/hinnastot [5.9.2012]

[6] Metso Minerals. (2011). Crushing and Screening Handbook (fifth edition).Tampere, Metso Minerals.

[7] Hulthén, E. (2010). Real-Time Optimization of Cone Crushers. Doctor of philosophy thesis. Göteborg, Sweden. Chalmers University of Technology. p.55.

[8] Hulthén, E., Evertsson, C. (2011). Real-time Algorithm for Cone Crushers Control with Two Variables. Minerals Engineering, Volume 24, Issue 9, pages 987-994.

[9] Itävuo, P., Vilkko, M., Jaatinen, A. (2012) Specific Energy Consumption – Based Cone Crusher Control. IFAC, Workshop on automation in the mining, mineral and metal industries, Gifu, Japan.

[10] Moshgbar, M., Bearman, R.A., Parkin, R. (1994). Optimum Control of Cone Crushers Utilizing an Adaptive Strategy for Wear Compensation. Minerals Engineering, Volume 8, Issues 4-5, pages 367-376.

[11] Itävuo, P. (2009). Dynamic Modelling of a Rock Crushing Process. Master of Science thesis. Tampere, Finland. Tampere University of Technology. p. 102.

[12] Al-Thaybat, S., Miles, N.J., Koh, T.S. (2006). Estimation of the size distribution of particles moving on a conveyor belt. Minerals Engineering, Volume 20, Issue 1, pages 72-83.

[13] Kaartinen, J. (2009). Machine Vision in Measurement and Control of Mineral Concentration Process. Helsinki, Finland. Helsinki University of Technology. Report. [Online] Available: http://lib.tkk.fi/Diss/2009/isbn9789512299553/isbn9789512299553.pdf [16.9.2012]

[14] Mkwelo, Simphiwe. (2004). A Machine Vision-based Approach to Measuring the Size Distribution of Rocks on a Conveyor Belt. Master of Science thesis. Cape Town, South Africa. University of Cape Town. p. 146.

[15] Taskinen, A. (2010). Size and Shape Distribution Estimation of Crushed Aggregate Using 3D Profile Measurement. Master of Science thesis. Tampere, Finland. Tampere University of Technology. p. 58.

[16] GTi Gasser. The Volume Rate Measuring system. [Online] Available: http://www.ultrasonic-measuring.com/fileadmin/templates/files/USMS_engl_tr.pdf [17.9.2012]

[17] Ohmart Vega. (2013). W4800 Radiation-Based Weight Systems for Conveyors. [Online] Available: http://www.ohmartvega.com/en/nuclear_weight_W4800.htm [28.1.2013]

[18] Yamazaki, T., Sakurai, Y., Ohnishi, H., Kobayashi, M., Kurosu, S. (2002). Continuous Mass Measurements in Checkweighers and Conveyor Belt Scales. [Online] Available: http://www.imeko.org/publications/tc3-2002/IMEKO-TC3-2002-001.pdf [6.3.2013]

[19] Pfreundt. (2010). Wheel Loader Scale Operating Principle and Equipment. [Online] Available: http://www.aldingercompany.com/Pfreundt_Wheel_Loader_Scales_Brochure.pdf [7.1.2013]

[20] Weighing-systems.com. (2005). Vehicle Weighing principles, [Online] Available: http://www.weighing-systems.com/TechnologyCentre/vehicleweigh.html [18.9.2012]

[21] Leonard, G.(2006). A weight bridge. [Online] Available: http://en.wikipedia.org/wiki/File:WeighBridge5500.JPG [14.2.2013]

[22] Aumala, O. (1998). Teollisuusprosessien Mittaukset. Published: Pressus, 1998. Tampere, Finland. p. 378.

[23] Shepherd, S.V. Siemens AG. (2009). Conveyor Belt Scales in Mining: Best Practice Installation, Calibration and Maintenance. IFACMMM 2009. p. 20.

[24] Seg Instruments AB. (2013). Bromma, Sweden. SEG ZH13 Belt Scale Datasheet. p. 2.

[25] Carlo Gavazzi. (2013). Energy Management, Compact Power Transducer datasheet. p. 9.

[26] McNutt, D.P. (1997). Chemical Rubber Co. Electrical Current Sensors. p. 15. [Online] Available: ftp://ftp.macnauchtan.com/Theory/Current.pdf [7.1.2013]

[27] Electricianeducation.com. (2010). Electrical power factor. [Online] Available: http://www.electricianeducation.com/theory/electrical_power_factor.htm [25.9.2012]

[28] SICK AG. (2011). Ruler E Reference Manual. Waldkirch, Germany. SICK AG. p. 87.

[29] Dorsch, R.G, Hausler, G. Herrmann, J.M. (1994). Laser triangulation: Fundamental Uncertainty in Distance Measurement. Applied Optics, Volume 33, Issue 7, pages 33-40.

[30] SICK AG. (2005). Ruler E Reference Manual. p. 12. [Online] Image: Available: ftp://ftp.SICKivp.se/download/Ruler%20E/Ruler_E_Reference_Manual.pdf [1.10.2012]

[31] SICK AG. (2005). Ruler E Reference Manual. p. 71. [Online] Image: Available: ftp://ftp.SICKivp.se/download/Ruler%20E/Ruler_E_Reference_Manual.pdf [1.10.2012]

[32] Endress & Hauser. (2011). Prosonic T FMU30 Technical Information. [Online] Available: http://www.endress.com/eh/home.nsf/#product/FMU30 [3.10.2012]

[33] Kyowa. (2011). Strain gauges for general stress measurement. Technical features about the Kyowa strain gauges. p. 8. [Online] Available: http://www.kyowa-ei.co.jp/eng/product/strain_gages/gages/kfg01.html [5.3.2013]

[34] Hoffmann, K. HBM GmbH. (2001). Applying the Wheatstone bridge Circuit, handbook. p.28.

[35] Orfanidis, S., J. (2007). Optimum Signal Processing, Second edition. New Jersey, USA. Rutgers University. p. 377.

[36] Larson, M., G., Bongzon, F. (2010). The Finite Element Method: Theory, Implementation, and Practice. Chalmers University of Technology and Umea University. p. 258.

[37] Lane, D. (2013). Online Statistics Education, Introduction to linear regression theory. [Online] Available: http://onlinestatbook.com/2/regression/intro.html [8.3.2013]

[38] Holmes, S. (2000) Stanford department of statistics. Root mean squared error theory. [Online] Available: http://www-stat.stanford.edu/~susan/courses/s60/split/node60.html [8.3.2013]

[39] Cameron, C., Windmeijer, F. (1996) An R-squared measure of goodness of fit for some common nonlinear regression models. Journal of Economics, Volume 77, Issue 2, pages 329-342.

[40] Bureau International des Poids et Mesures. (2008). Evaluation of measurement data – Guide to the expression of uncertainty in measurement. Propagation of uncertainty. [Online] Available: http://www.bipm.org/en/publications/guides/gum.html [11.3.2013]

APPENDIX A

Original measurement signals of the power transducer, laser profilometer, ultrasonic sensor, strain gauges and belt scale.

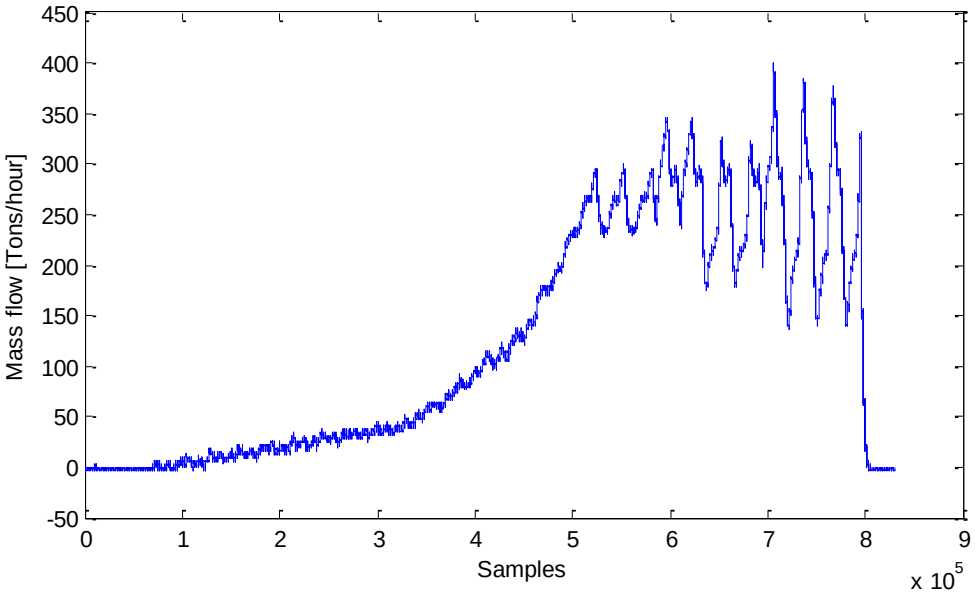

Figure 1. *The original measurement signal of the belt scale*

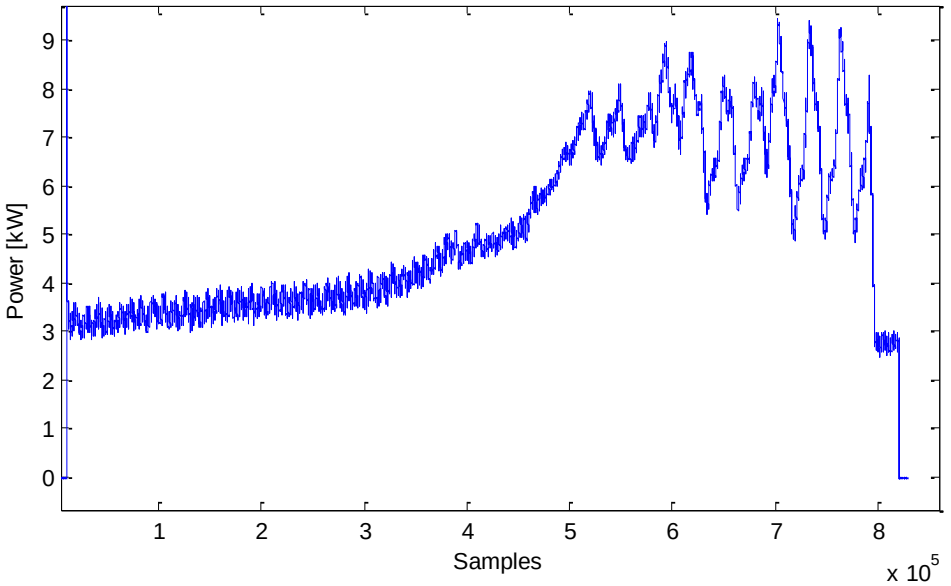

Figure 2. *The original measurement signal of the power transducer*

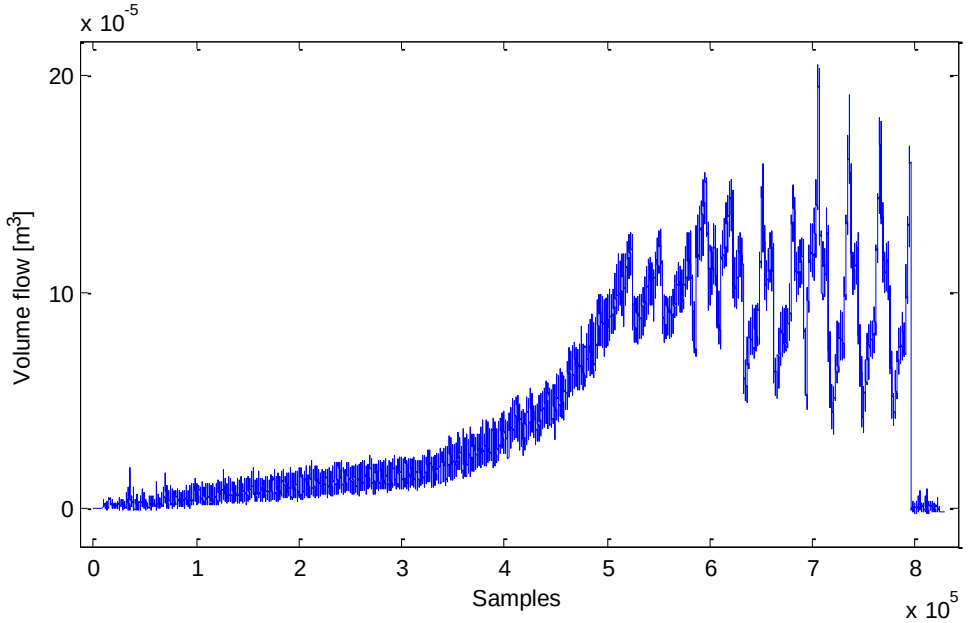

Figure 3. *The original measurement signal of the laser profilometer*

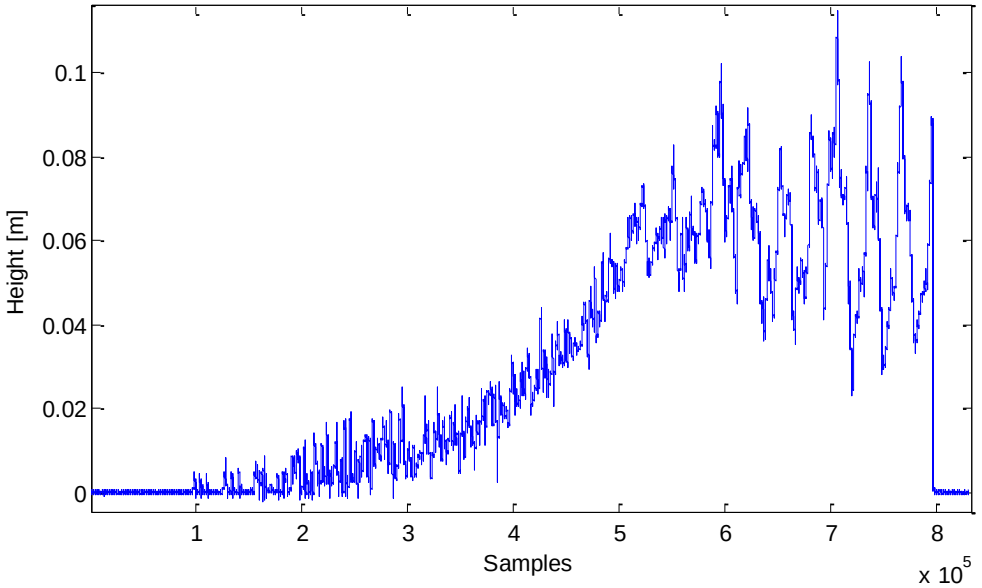

Figure 4. *The original measurement signal of the ultrasonic sensor*

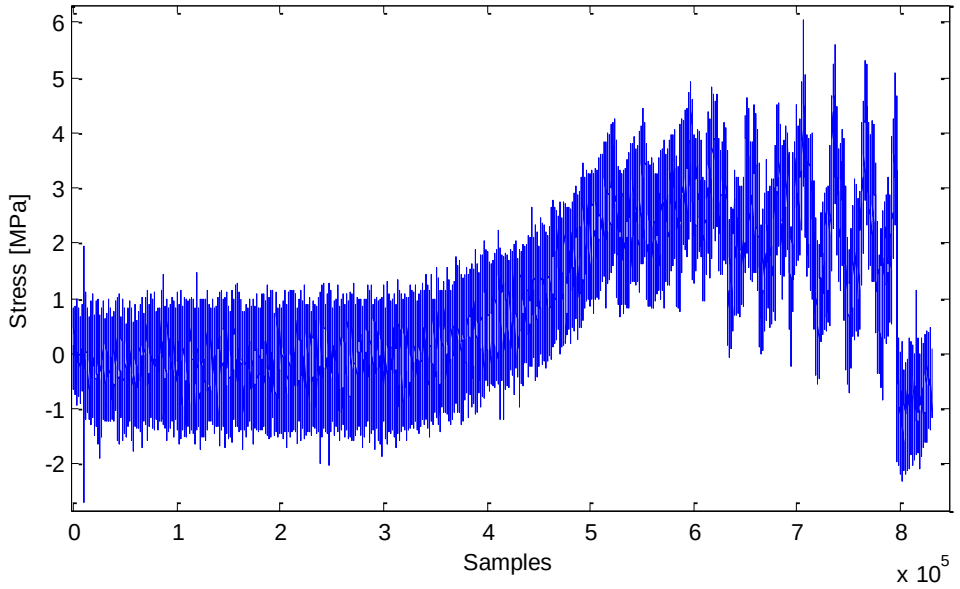

Figure 5. *The original measurement signal of the strain gauge one*

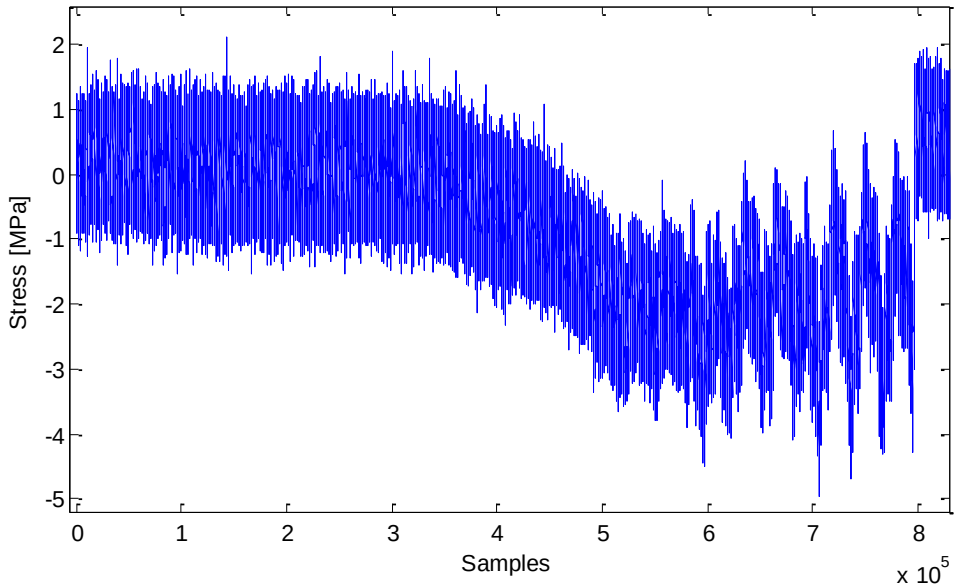

Figure 6. *The original measurement signal of the strain gauge two*

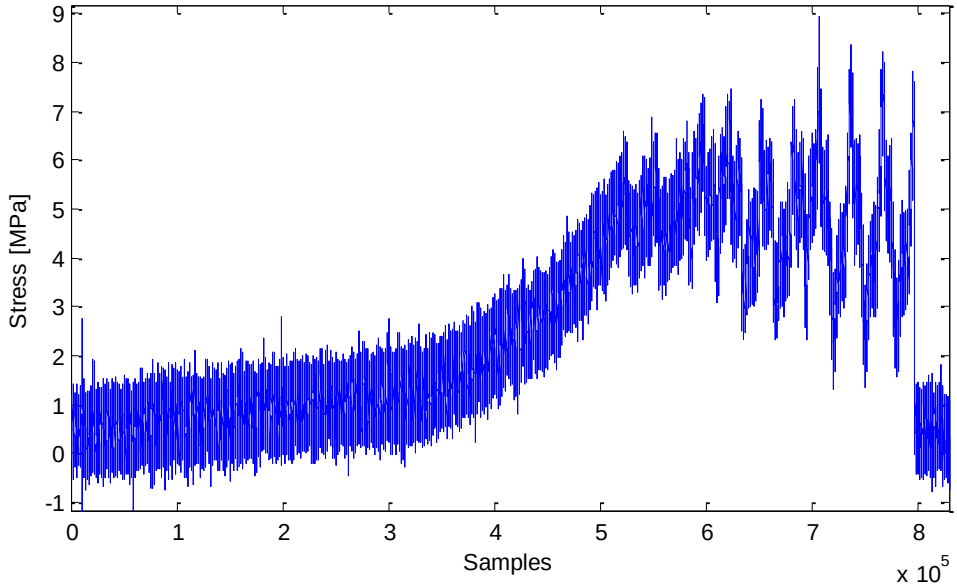

Figure 7. *The original measurement signal of the strain gauge three*

APPENDIX B

The linear regression models of the online mass flow sensors fitted to the reference mass flow measurement of the belt scale. All the signals are filtered with a moving average filter of 500 samples for better visualisation.

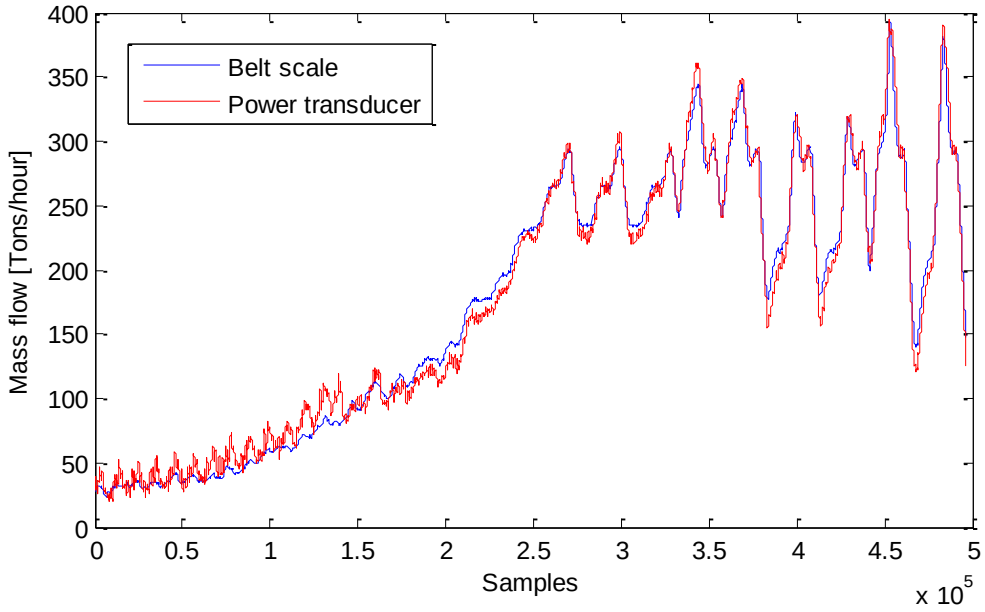

Figure 1. *The linear regression model estimate of the power transducer and the reference mass flow measurement of the belt scale.*

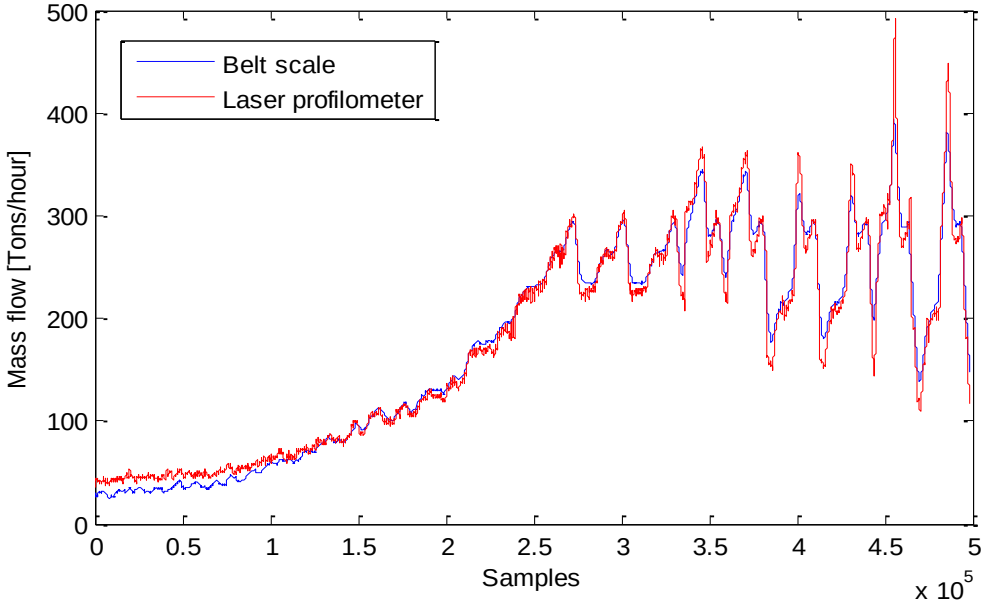

Figure 2. *The linear regression model estimate of the laser profilometer and the reference mass flow measurement of the belt scale.*

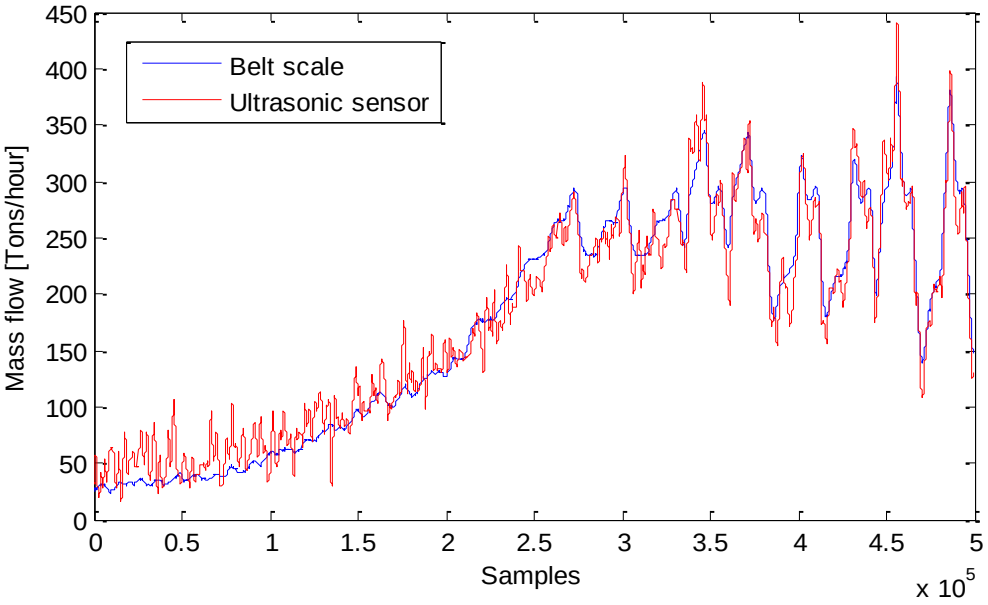

Figure 3. *The linear regression model estimate of the ultrasonic sensor and the reference mass flow measurement of the belt scale.*

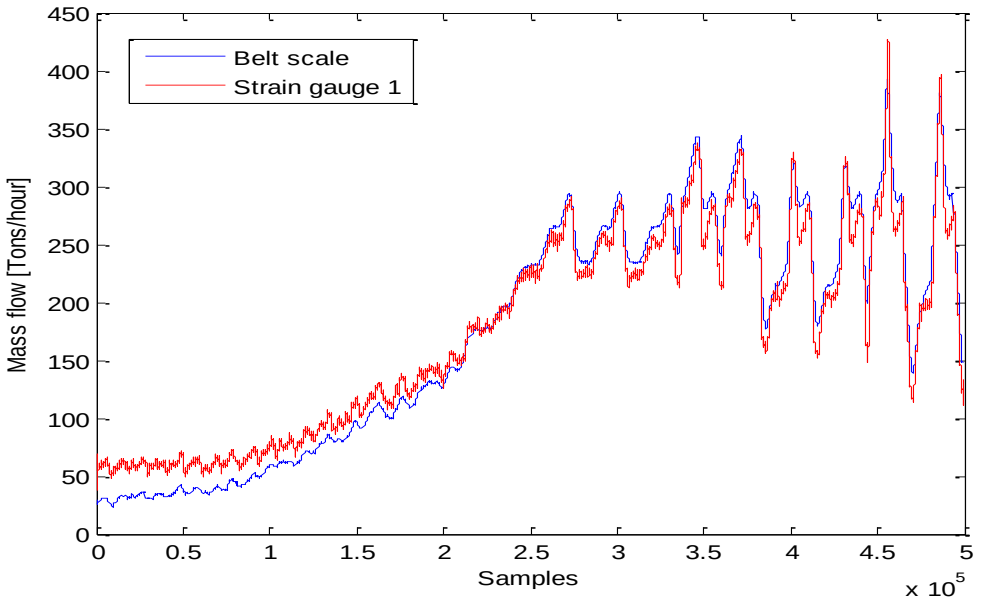

Figure 4. *The linear regression model estimate of the strain gauge one and the reference mass flow measurement of the belt scale.*

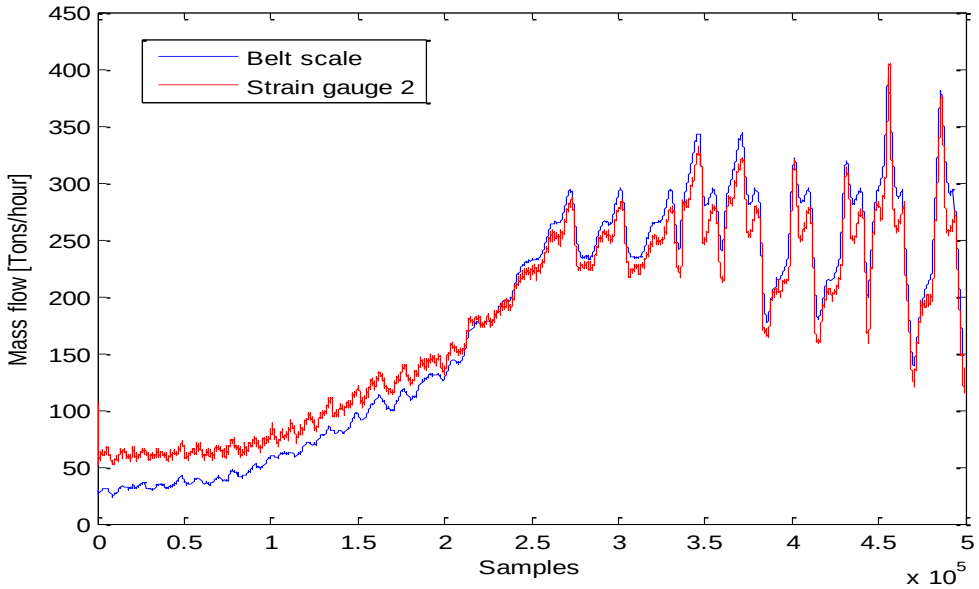

Figure 5. *The linear regression model estimate of the strain gauge two and the reference mass flow measurement of the belt scale.*

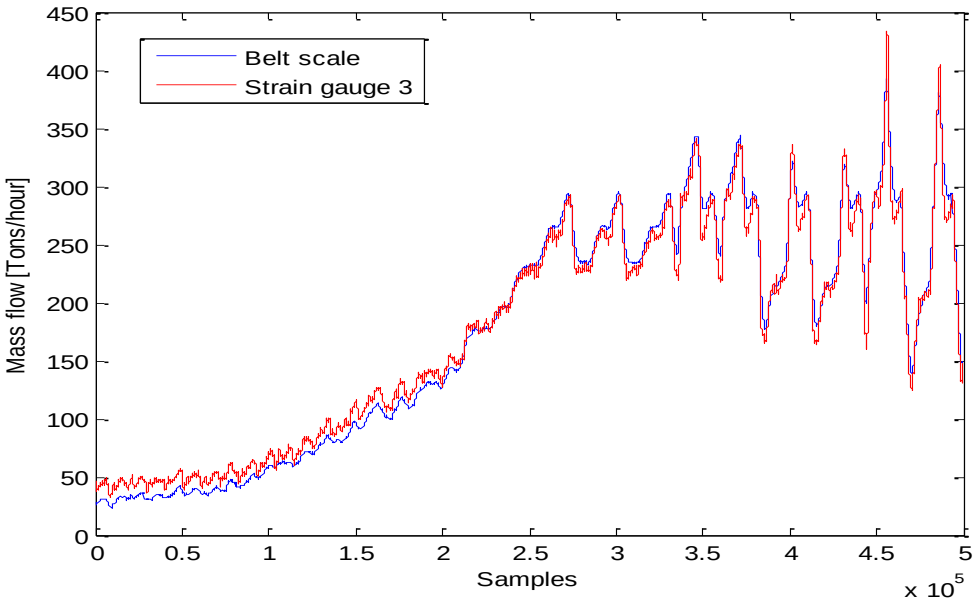

Figure 6. *The linear regression model estimate of the strain gauge three and the reference mass flow measurement of the belt scale.*

APPENDIX C

The histograms of residuals for the online mass flow sensors used in this work.

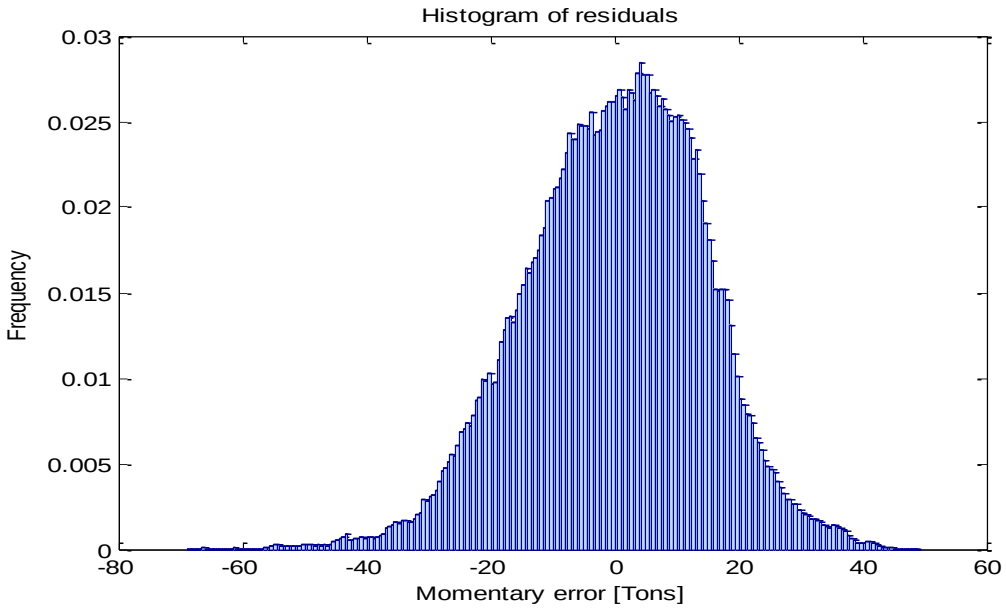

Figure 1. *The distribution of residuals between the measurement signals of the power transducer and the belt scale.*

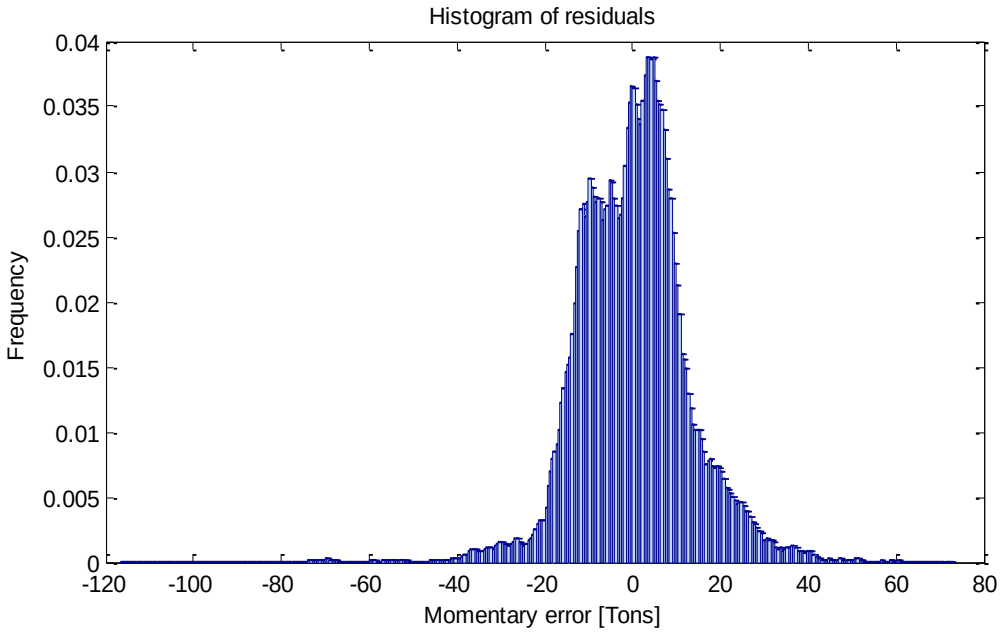

Figure 2. *The distribution of residuals between the measurement signals of the laser profilometer and the belt scale.*

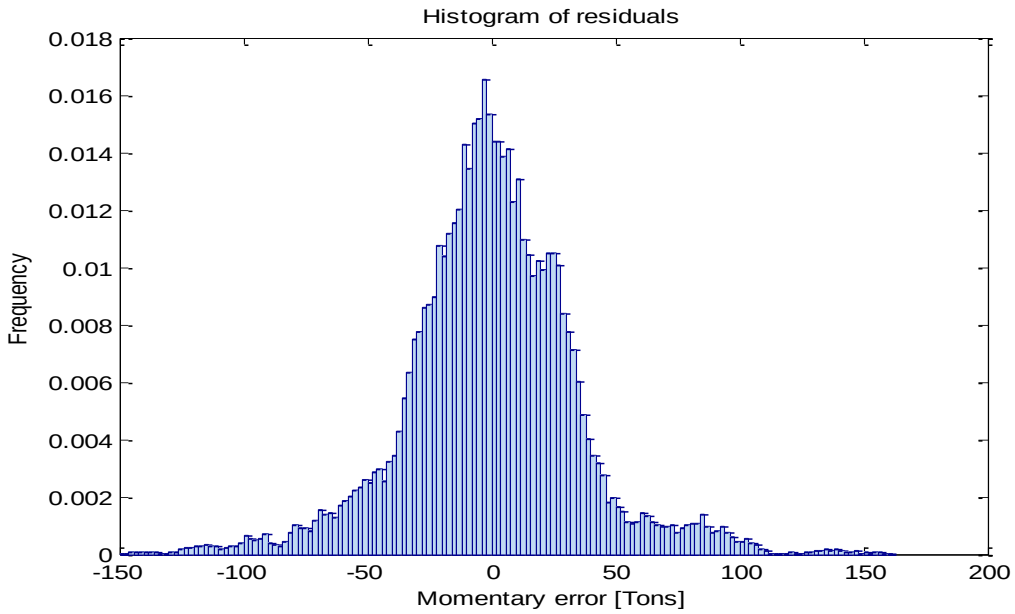

Figure 3. *The distribution of residuals between the measurement signals of the ultrasonic sensor and the belt scale.*

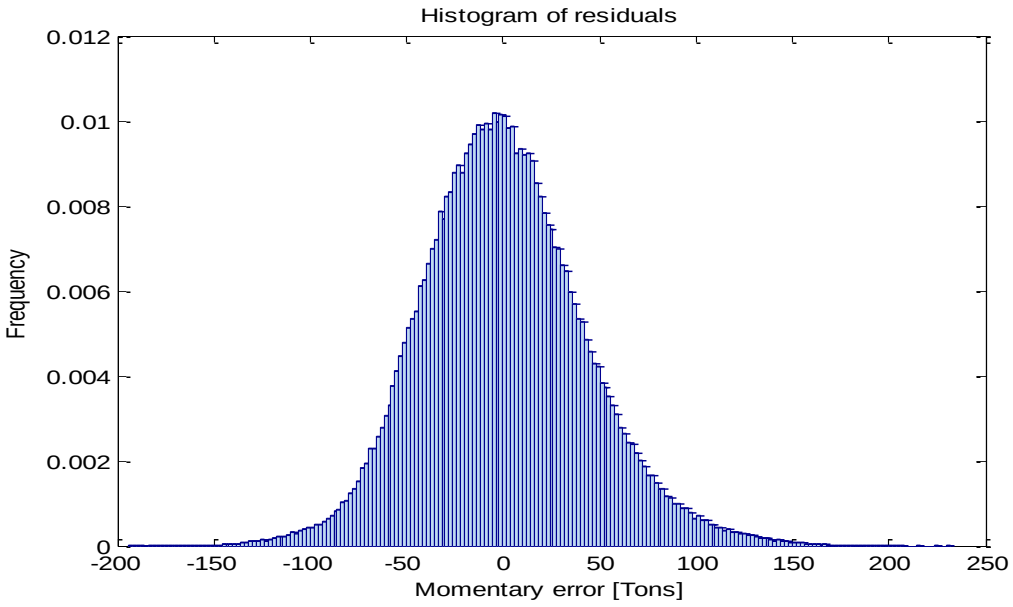

Figure 4. *The distribution of residuals between the measurement signals of the strain gauge one and the belt scale.*

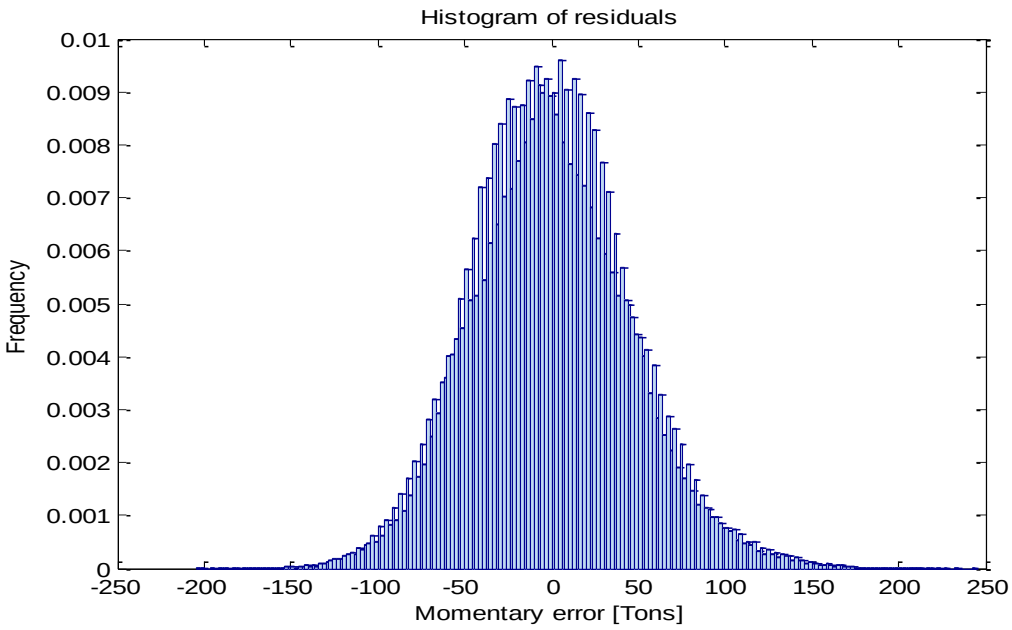

Figure 5. *The distribution of residuals between the measurement signals of the strain gauge two and the belt scale.*

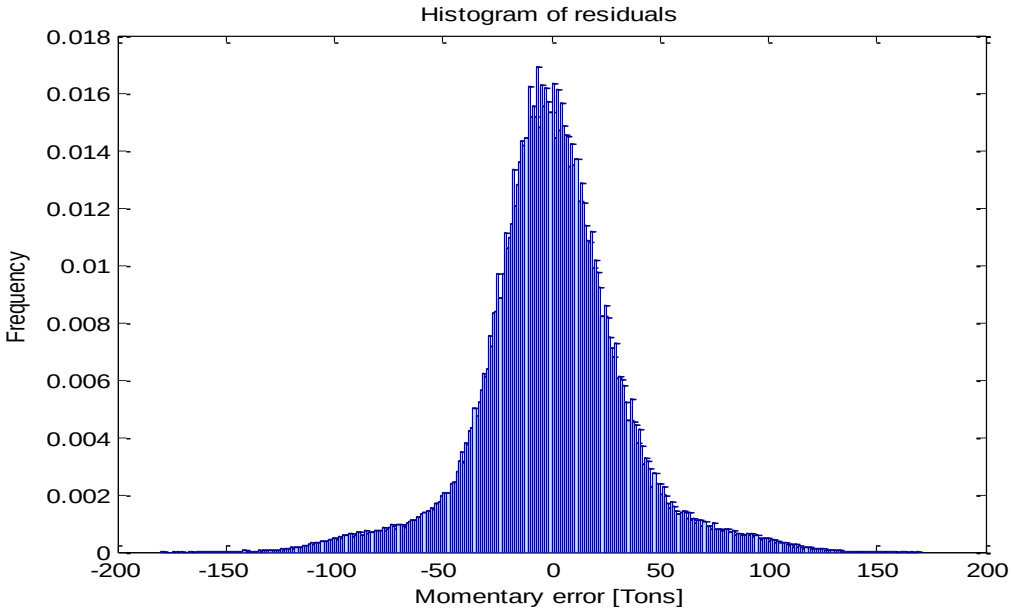

Figure 6. *The distribution of residuals between the measurement signals of the strain gauge three and the belt scale.*